

CHAPTER IV RESULTS AND DISCUSSION

4.1 Production of Bacterial Cellulose and Bacterial Cellulose Composites

Acetobacter xylinum strain TISTR 975, statically inoculates in a suitable culture medium consisting of D-glucose 4 %w/v and yeast extract 2 % w/v at 30 °C, produced bacterial cellulose and formed a thick gelatinous pellicle at the air-liquid interface of the culture medium within 1-8 days as shown in Figure 4.1

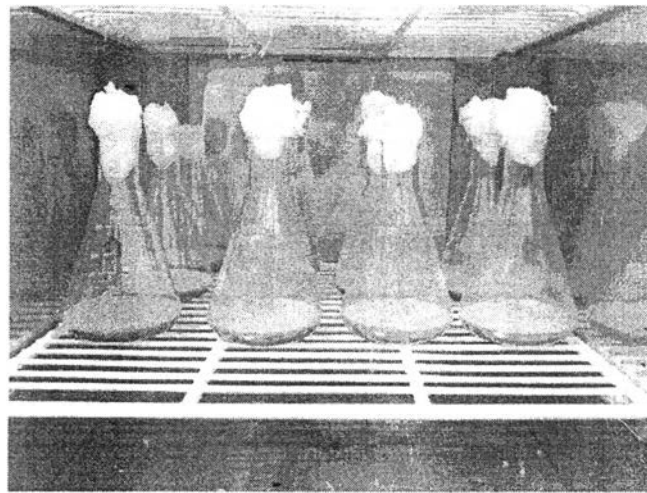


Figure 4.1 Cultivation of *Acetobacter xylinum* strain TISTR 975 : forming of the gelatinous bacterial cellulose pellicles.

The formation of the bacterial cellulose took place on the upper site of the cellulose layer. Bacterial cells increased their population by consumption of oxygen and D-glucose, initially dissolved in the culture medium, as carbon source. During growth and production of bacterial cellulose, the bacterial cells were gradually entrapped in the pellicle. As long as the system was kept unshaken, the bacterial cellulose pellicle suspended on the surface of culture medium.

After a certain cultivation time of *Acetobacter xylinum* strain TISTR 975, the gelatinous white pellicle of bacterial cellulose at the surface of culture medium was harvested. For purification, the bacterial cellulose pellicle was boiled in a

sodium hydroxide solution (NaOH) 1.0 %w/v for 2 hrs (3 times) to eliminate *Acetobacter xylinum* cells, protein which is a by-product during the bacterial metabolism and the culture medium that entrapped within the bacterial cellulose pellicle. After that, neutralization with acetic acid solution 1.5 %w/v for 30 min, followed by immersing in distilled water until neutral pH was obtained. Figure 4.2 (a) shows the yellow-translucent pellicle of untreated bacterial cellulose became a white-transparent pellicle after purification figure 4.2 (b).

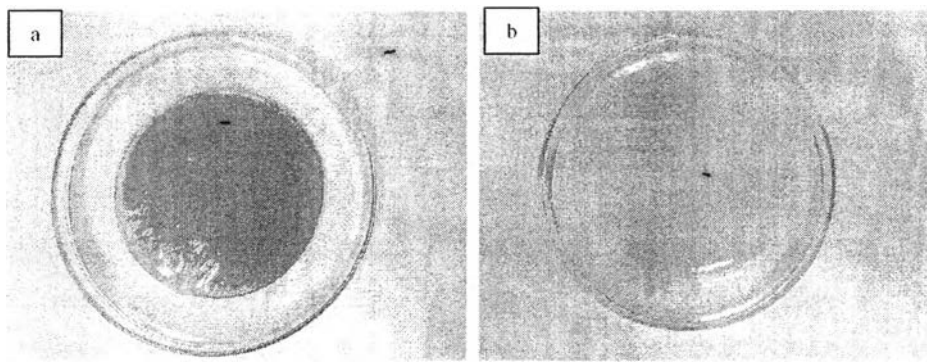


Figure 4.2 Purification of bacterial cellulose. (a) before purification and (b) after purification.

The purification result was also confirmed by using SEM images. Figure 4.3 (a) shows surface morphology of untreated bacterial cellulose compared with the NaOH-treated bacterial cellulose (figure 4.3 (b)). After purification, the random assembly of ultrafine three dimensional non-woven network structure of nanofibrils which constructs high porosity structure was obtained. It can be explained that the bacterial cells, protein, and any component of the culture medium were completely eliminated by NaOH treatment.

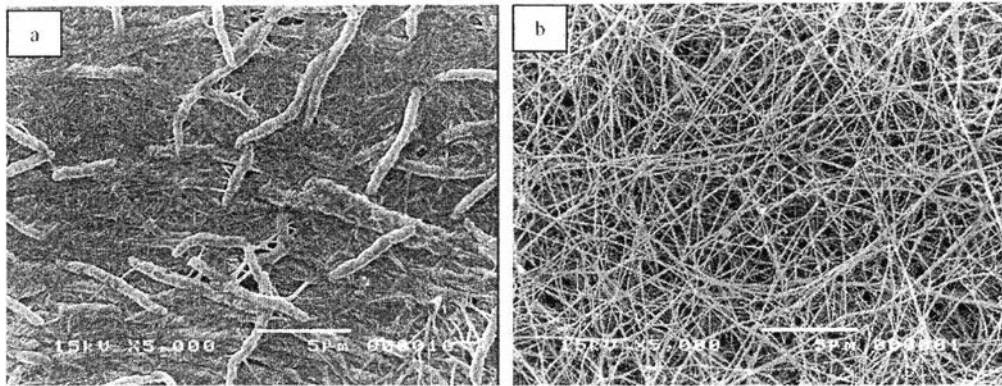
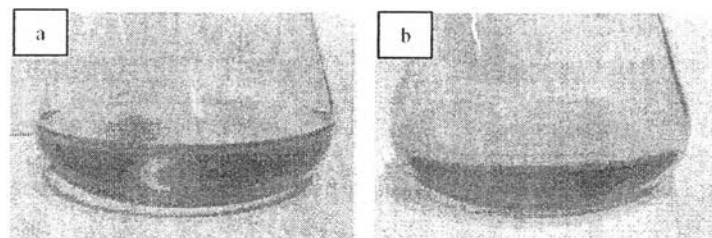


Figure 4.3 SEM images show the surface morphology of bacterial cellulose, (a) before purification and (b) after purification.

4.2 Effect of Cultivation Time on Thickness and Dry Weight of Bacterial Cellulose Pellicle

Figure 4.4 shows the thickness of bacterial cellulose pellicle under different cultivation time 1-8 days and figure 4.5 shows the relationship between thickness of bacterial cellulose and cultivation time. From the results, after 1 day of cultivation, the thin gelatinous bacterial cellulose was formed at the surface of culture medium. The thickness of bacterial cellulose pellicle increased rapidly for 1-4 days. After 4 days, the thickness of bacterial cellulose pellicle increased slowly. In addition, dry weight of bacterial cellulose also increased rapidly for 1-4 days. After 4 days, dry weight of bacterial cellulose increased slowly as shown in Figure 4.6



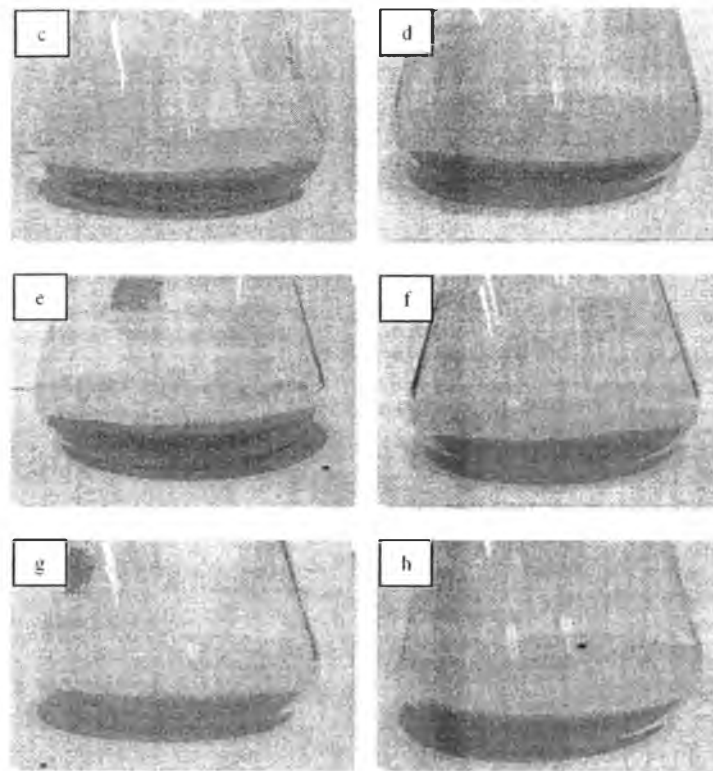


Figure 4.4 Bacterial cellulose pellicle produced by *Acetobacter xylinum* TISTR 975 under different cultivation time (a-h) 1-8 days, respectively.

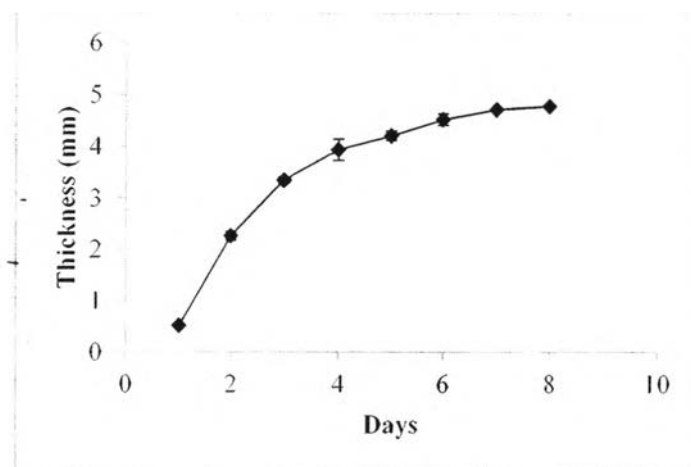


Figure 4.5 Comparison of thickness of bacterial cellulose pellicle under different cultivation time (1-8 days).

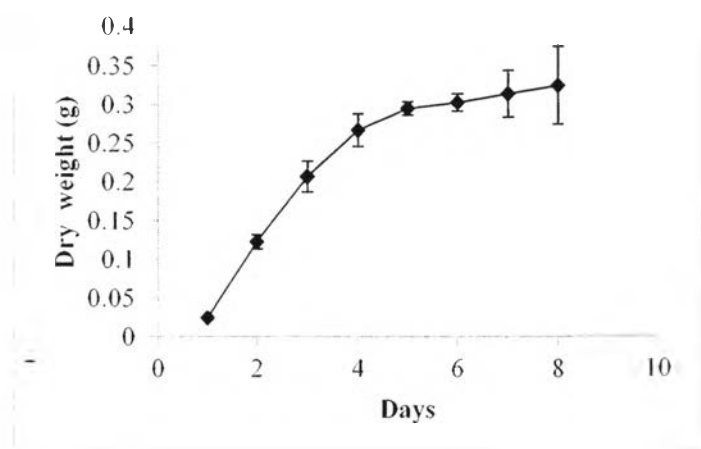


Figure 4.6 Comparison dry weight of bacterial cellulose pellicle under different cultivation time (1-8 days).

From the results, the thickness and dry weight of bacterial cellulose increased slowly after 4 days, then the optimum cultivation time is 4 days for production of pure bacterial cellulose.

4.3 Fourier Transform Infrared Spectroscopy (FTIR)

The chemical functional groups of bacterial cellulose (BC) were examined by using fourier transform infrared spectroscopy (FTIR). The FTIR spectra was detected at wavenumber ranging from 4000 to 650 cm^{-1} . Figure 4.7 shown FTIR spectra of pure BC. The peak at wavenumber 3343 cm^{-1} corresponds to the OH stretching, the peak at 2895 cm^{-1} corresponds to the C-H stretching and the peak at 1032 cm^{-1} corresponds to the C-O stretching.

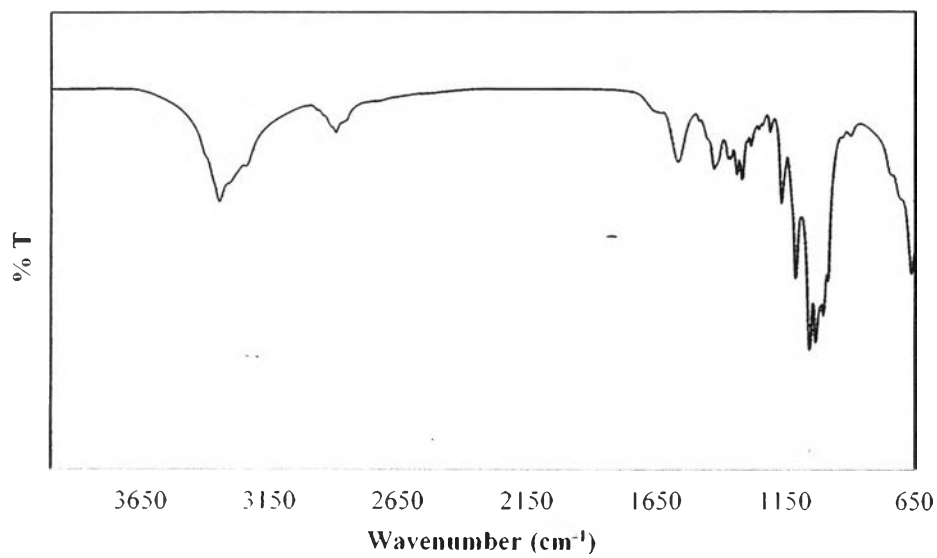


Figure 4.7 FTIR spectra of pure BC.

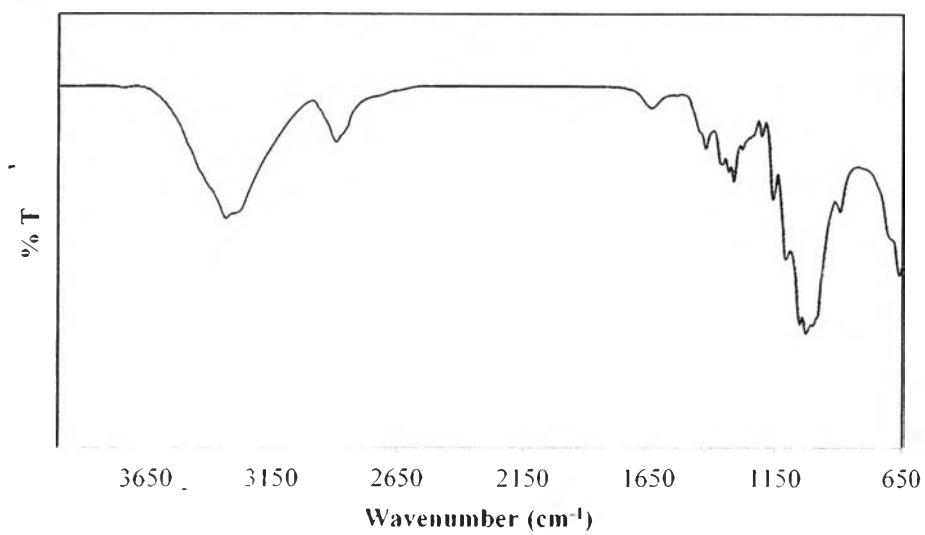


Figure 4.8 FTIR spectra of lenin fabric.

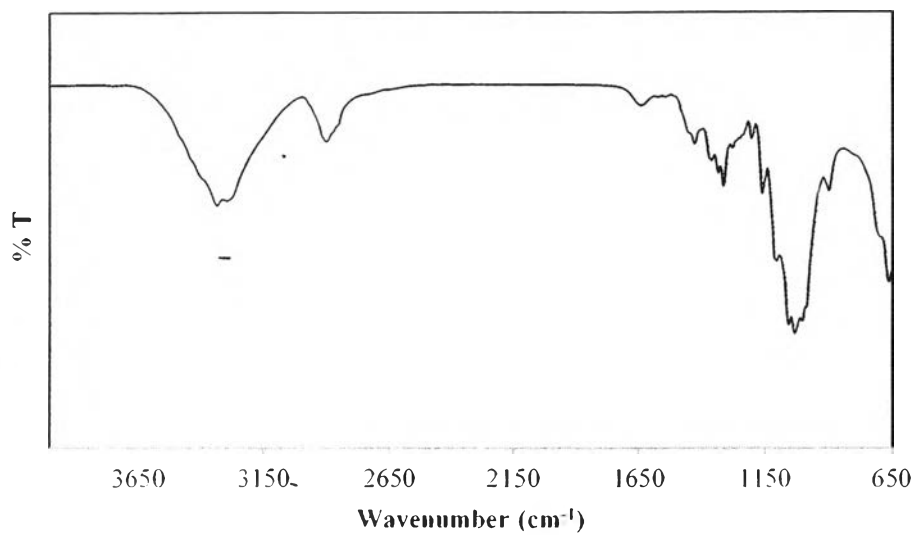


Figure 4.9 FTIR spectra of cotton fabric.

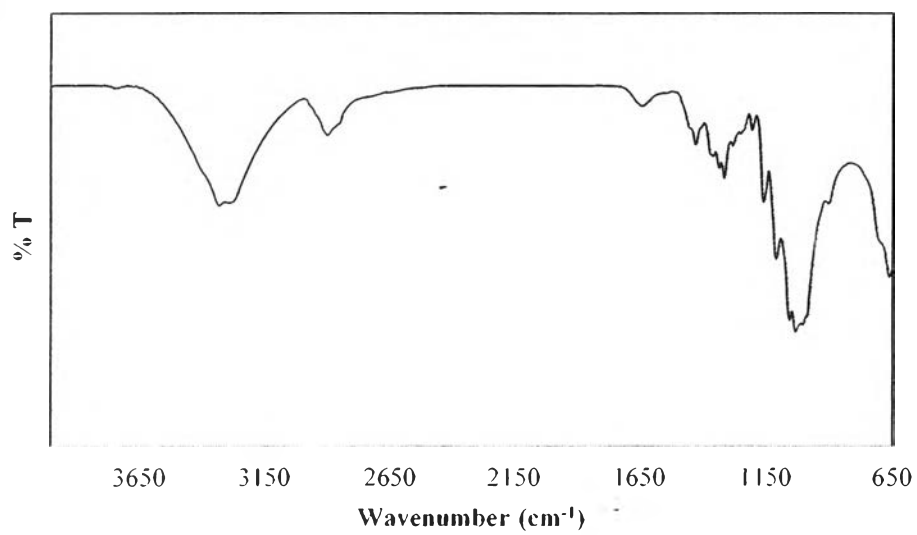


Figure 4.10 FTIR spectra of filter cloth fabric.

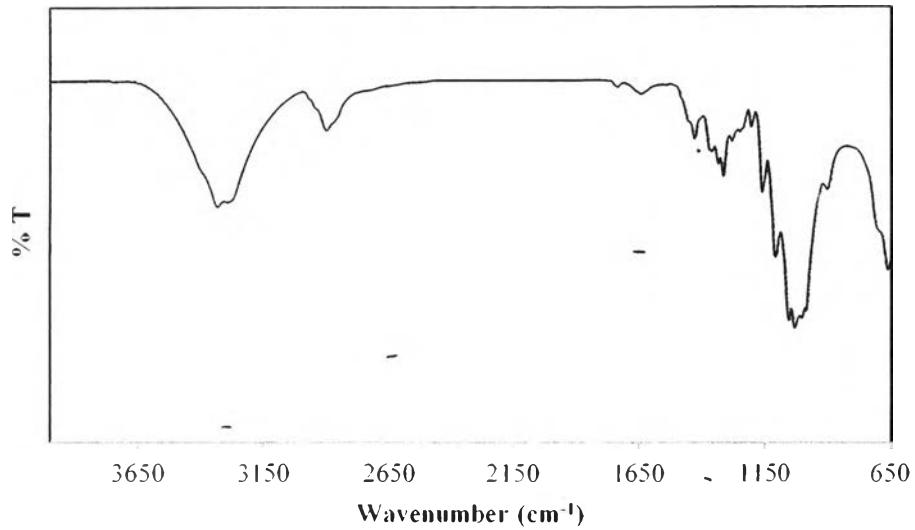


Figure 4.11 FTIR spectra of muslin fabric.

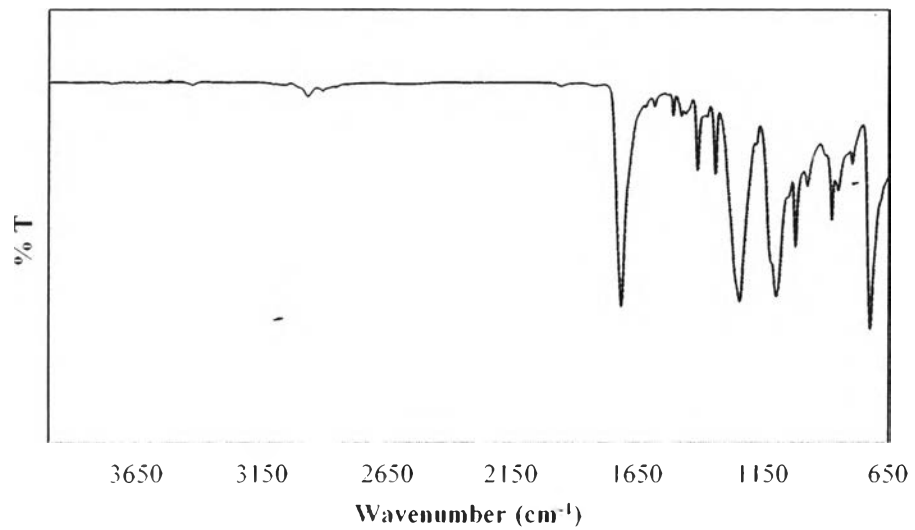


Figure 4.12 FTIR spectra of polyester fabric.

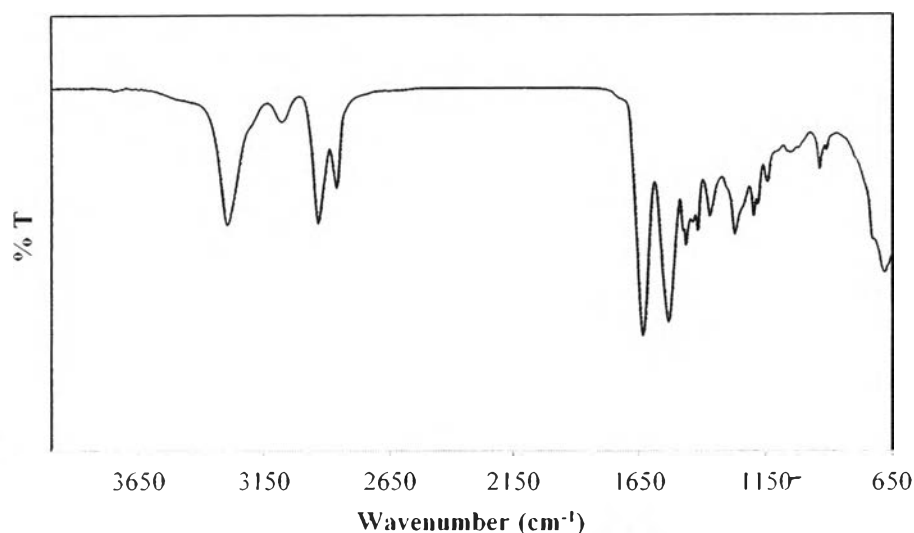


Figure 4.13 FTIR spectra of nylon mesh.

Figure 4.8 shows FTIR spectra of lenin fabric. The spectra shows the peak at wavenumber 3331 cm^{-1} corresponds to the OH stretching, the peak at 2899 cm^{-1} corresponds to the C-H stretching and the peak at 1029 cm^{-1} corresponds to the C-O stretching.

Figure 4.9 shows FTIR spectra of cotton fabric. The spectra shown the peak at wavenumber 3336 cm^{-1} corresponds to the OH stretching, the peak at 2900 cm^{-1} corresponds to the C-H stretching and the peak at 1029 cm^{-1} corresponds to the C-O stretching.

Figure 4.10 shows FTIR spectra of filter cloth fabric. The spectra shown the peak at wavenumber 3331 cm^{-1} corresponds to the OH stretching, the peak at 2899 cm^{-1} corresponds to the C-H stretching and the peak at 1027 cm^{-1} corresponds to the C-O stretching.

Figure 4.11 shows FTIR spectra of muslin fabric. The spectra shown the peak at wavenumber 3333 cm^{-1} corresponds to the OH stretching, the peak at 2899 cm^{-1} corresponds to the C-H stretching and the peak at 1029 cm^{-1} corresponds to the C-O stretching. From the FTIR spectra, can be concluded that lenin, cotton filter cloth and muslin fabrics were polyether.

Figure 4.12 shows FTIR spectra of polyester fabric. The spectra shown the peak at wavenumber 1712 cm^{-1} corresponds to the C=O stretching, the two peak at 1095 cm^{-1} and 1242 cm^{-1} corresponds to the C-O stretching.

Figure 4.13 shows FTIR spectra of nylon mesh. The spectra shown the peak at wavenumber 3298 cm^{-1} corresponds to the NH stretching, the peak at 2932 cm^{-1} corresponds to the C-H stretching, the peak at 1633 cm^{-1} corresponds to the C=O stretching and the peak at 1532 cm^{-1} correspond to the NH bending. Then, nylon mesh was polyamide.

4.4 Morphology of Bacterial Cellulose

SEM images of the surface morphology and cross sectional of the pure BC as shown in figure 4.14. Figure 4.14 (a). SEM image of surface morphology of pure BC shows the random assembly of ultrafine three dimensional non-woven network structure of nanofibrils which constructs high the porosity structure. Figure 4.14 (b), SEM image of the cross sectional morphology of pure BC shows the interconnection of fibrils linked between the multilayer of cellulose network structure. This result confirms the mechanism of formation of the bacterial cellulose pellicle, only bacterial exist in the vicinity of the surface of culture medium can be associate with oxygen. Production of bacterial cellulose pellicle occurs downwards.

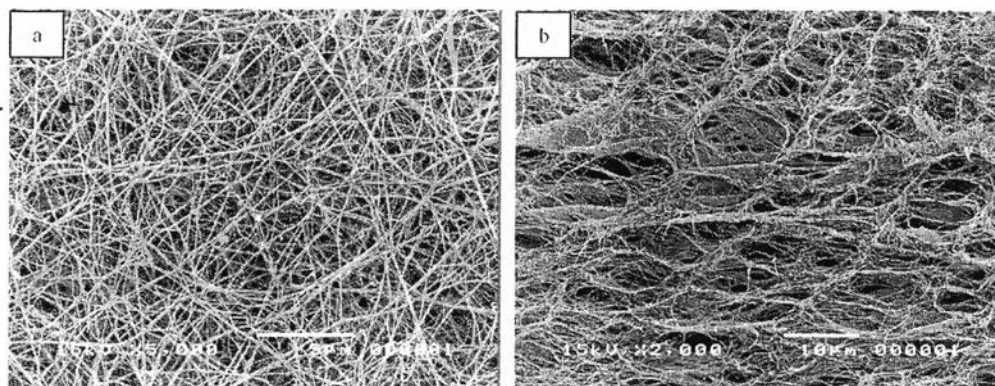


Figure 4.14 SEM images of bacterial cellulose, (a) surface and (b) cross section morphology.

For preparation porous supporting fabric embedded bacterial cellulose composites, the effect of chemical functional groups of fabric on the cell attachment of bacterial cells was investigated by using different types of porous supporting fabrics. The porous supporting fabrics that used in this research consist of lenin, cotton, filter cloth, muslin, shefong and nylon mesh. Cotton, muslin, lenin and filter cloth were polyether, shefong was polyester and nylon mesh was polyamide. The surface morphology of fabrics was shown in figure 4.15.

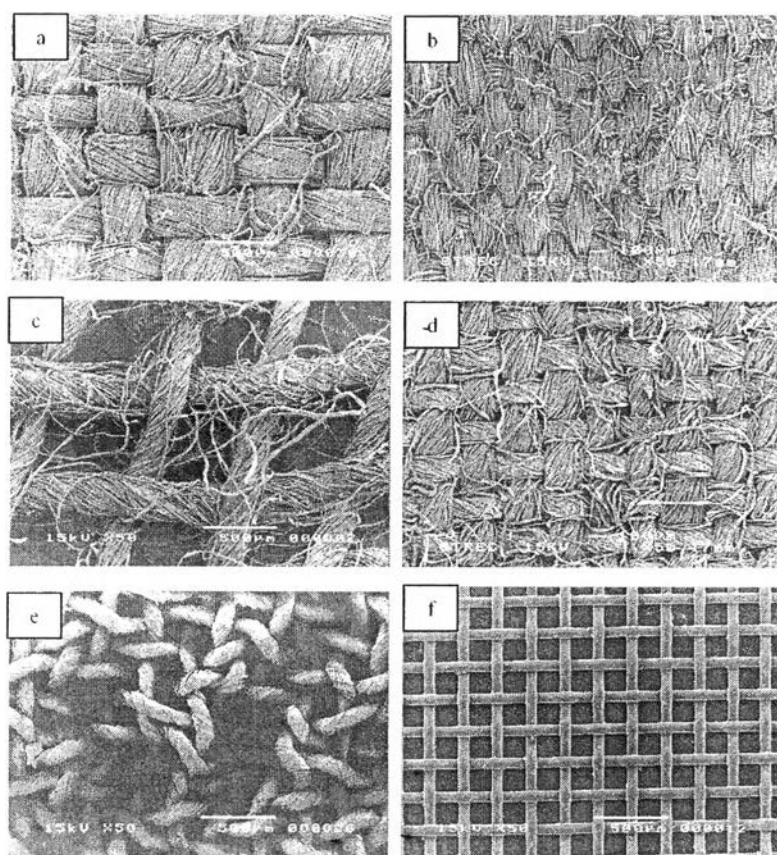


Figure 4.15 Surface morphology of (a) lenin, (b) cotton, (c) filter cloth, (d) muslin, (e) polyester and (f) nylon mesh, respectively.

The porous supporting fabrics show the woven structure but the woven fibers density was difference. Lenin and cotton have higher fibers density than other fabrics. Filter cloth, muslin, polyester and nylon mesh have lower fibers density, especially filter cloth. Lenin was made from flax fibers. Cotton, filter cloth and

muslin were made from cotton fibers. Polyester and nylon mesh were made from synthesis.

Production of BC composites, the cross section morphology (figure 4.17 a-f), the interaction between bacterial cellulose fibrils and fabrics were observed. In addition, the surface morphology (figure 4.16) and cross sectional morphology (figure 4.17 g-l) were the same as those of pure BC but the fibrillar structures in the composite were denser than that of pure BC, especially in the BC/Nylon composites. Using porous supporting fabric could lead to the increasing of the number of cell attachment of bacterial cells on the fabrics, resulting in the increasing of the production yields of bacterial cellulose when compared with pure BC. Since the chemical structure of nylon mesh is polyamide consisting of CONH groups, which is the same as peptide bond of protein, nylon mesh had better compatibility with bacterial cell than the other fabrics as well as had higher production yields.

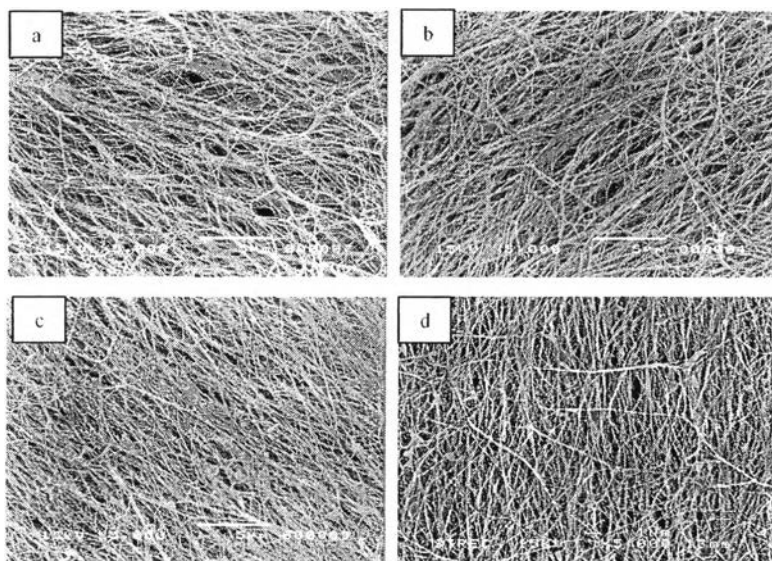


Figure 4.16 Surface morphology of (a) BC/Lenin, (b) BC/Cotton, (c) BC/Filter cloth, (d) BC/Muslin, (e) BC/Polyester and (f) BC/Nylon composites, respectively.

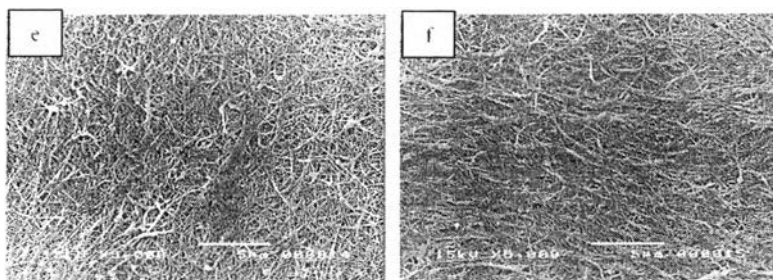


Figure 4.16 (Cont.) Surface morphology of (a) BC/Lenin, (b) BC/Cotton, (c) BC/Filter cloth, (d) BC/Muslin, (e) BC/Polyester and (f) BC/Nylon composites, respectively.

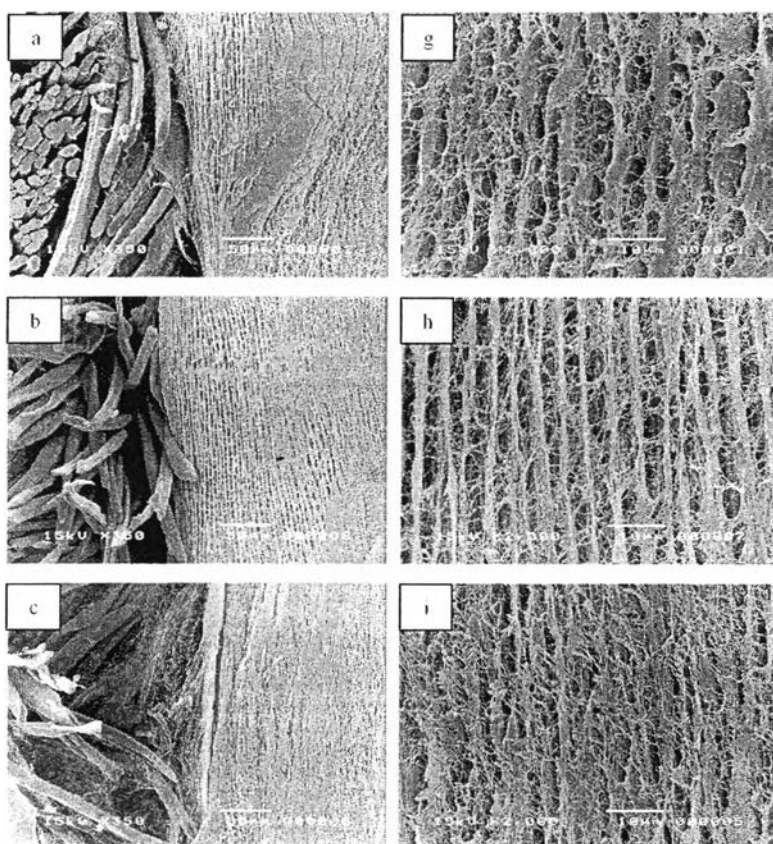


Figure 4.17 (a-f) shown cross sectional morphology and (g-l) shown only BC part in BC/Lenin, BC/Cotton, BC/Filter cloth, BC/Muslin, BC/Polyester and BC/Nylon, respectively.

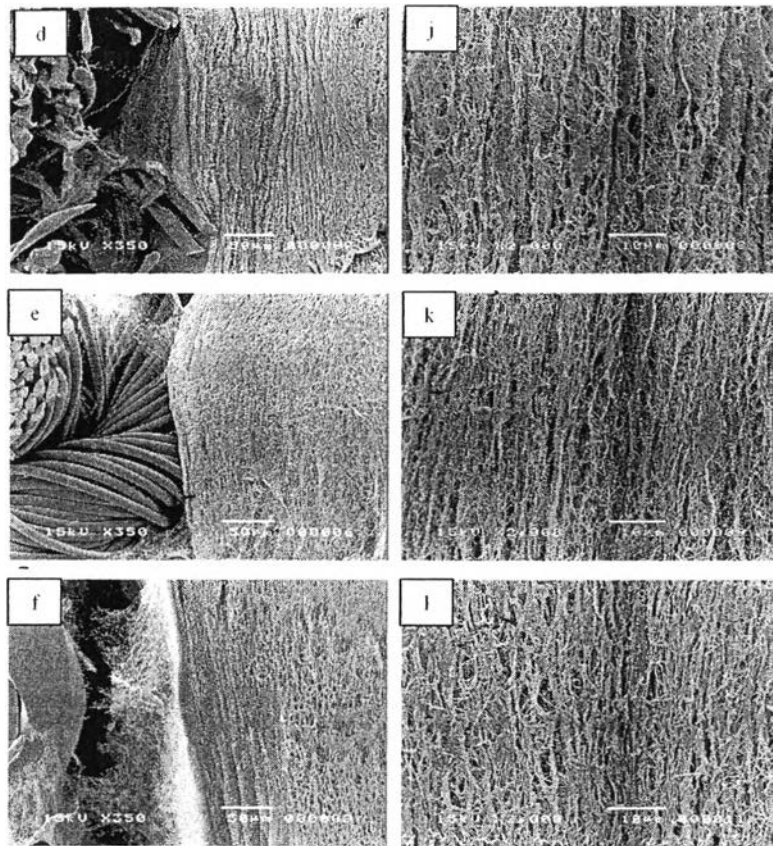


Figure 4.17 (Cont.) (a-f) shown cross sectional morphology and (g-l) shown only BC part in BC/Lenin, BC/Cotton, BC/Filter cloth, BC/Muslin, BC/Polyester and BC/Nylon, respectively.

To observe the interaction between BC fibrils and fabric fibres, BC pellicle was removed out of the fabrics. The surface morphology of fabrics after removed BC as shown in figure 4.18. From the SEM images, confirmed that the BC fibrils directly interacted with the fabric fibres and held them together. Although the BC fibrils density was lower than those produces at the surface due to removing, the ultrafine three dimensional non-woven network structure of nanofibrils was formed that connected each fabric fibres. It is suggested that this network structure contributes to the adhesion of BC pellicle to the fabric surface.

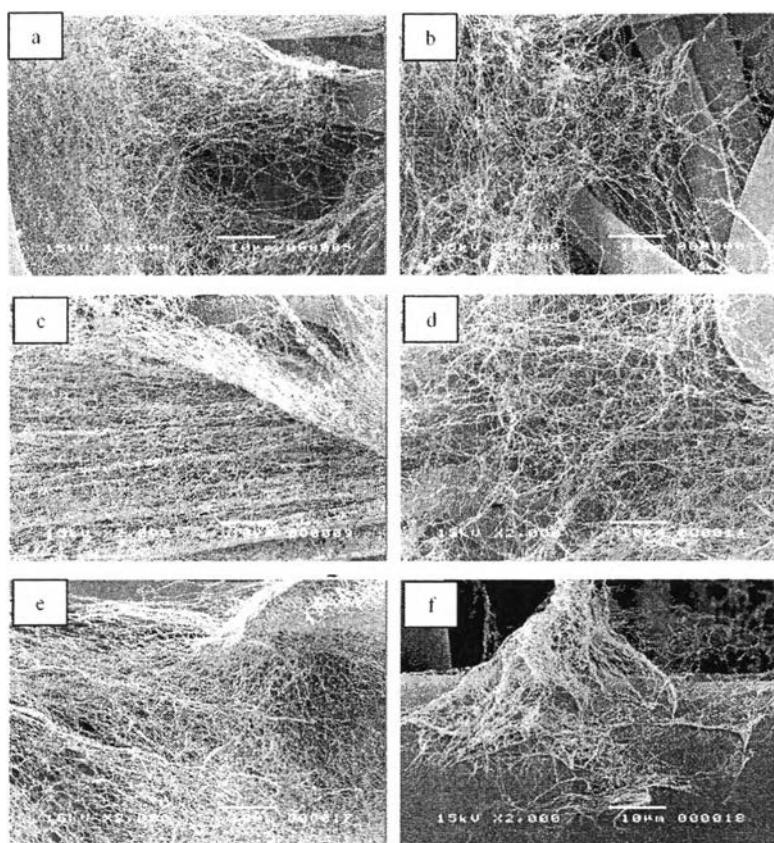


Figure 4.18 The interaction between BC fibrils and fabrics (a) lenin, (b) cotton, (c) filter cloth, (d) muslin, (e) polyester and (f) nylon mesh fabrics, respectively.

4.5 Dielectric Barrier Discharge (DBD) Plasma Treatment Fabrics

Dielectric barrier discharge (DBD) plasma is widely used to modify the surface properties of polymer in many applications such as improving the adhesion of coating to polymers, printing and biomedical application. The interactions of plasma with polymer surface are physical bombardment and chemical reaction. Surface roughness and surface area were increased by etching polymer surface. In this point, can be improve cell attachment on fabrics, that the advantages of the production of fibrils. Figure (4.19-4.24) show the effect of DBD plasma treatment time on the surface roughness of lenin, cotton, filter cloth, muslin, polyester and nylon mesh fabrics, respectively. For lenin, cotton, filter cloth and muslin fabrics, DBD plasma treatment time 30 seconds, the surface roughness of fabrics was not

different from non DBD plasma treatment. In contrast, polyester and nylon mesh fabrics, micro pits were formed on the surface of fabrics leading to increase the surface roughness of fabrics. When treatment time increasing of 2 minutes, micro pits were formed more than that in 30 seconds. For treatment time 3 minutes, the surface roughness was slightly increased when compared with DBD plasma treatment time 2 minutes. In this research, DBD plasma treatment time of 2 minutes was chosen because treatment time too long could lead to damage the structure of fabrics.

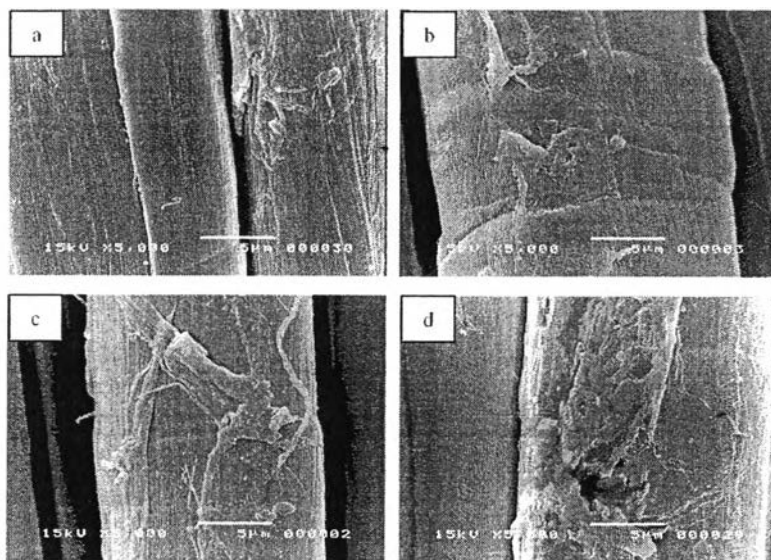


Figure 4.19 The effect of DBD plasma treatment time on the surface roughness of lenin fabric, (a) non DBD plasma treated fabric, (b-d) DBD plasma treated fabric 30 seconds, 2 min and 3 min, respectively.

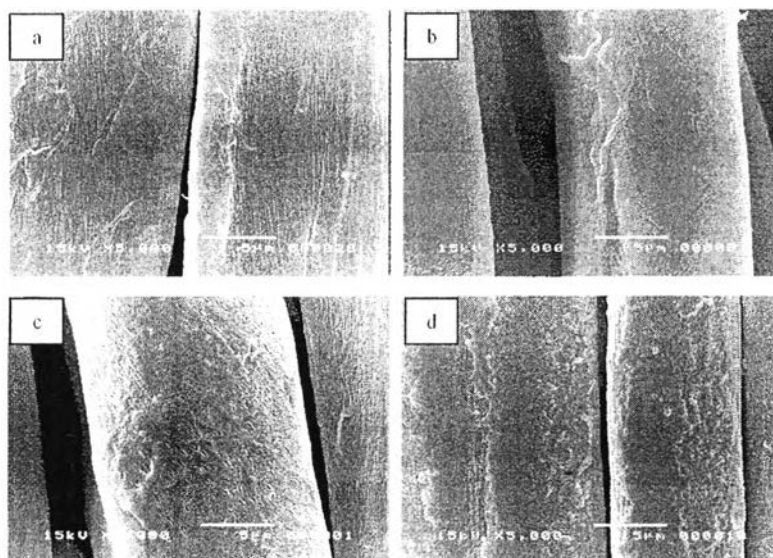


Figure 4.20 The effect of DBD plasma treatment time on the surface roughness of cotton fabric, (a) non DBD plasma treated fabric, (b-d) DBD plasma treated fabric 30 seconds, 2 min and 3 min, respectively.

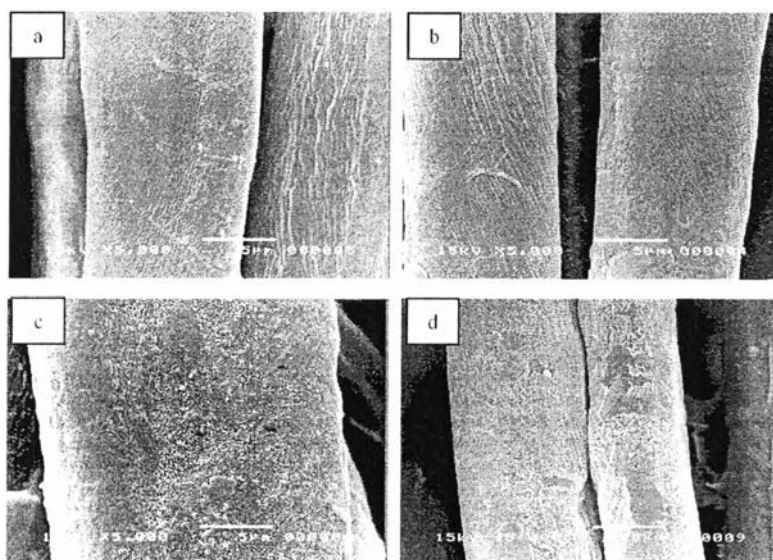


Figure 4.21 The effect of DBD plasma treatment time on the surface roughness of filter cloth fabric, (a) non DBD plasma treated fabric, (b-d) DBD plasma treated fabric 30 seconds, 2 min and 3 min, respectively.

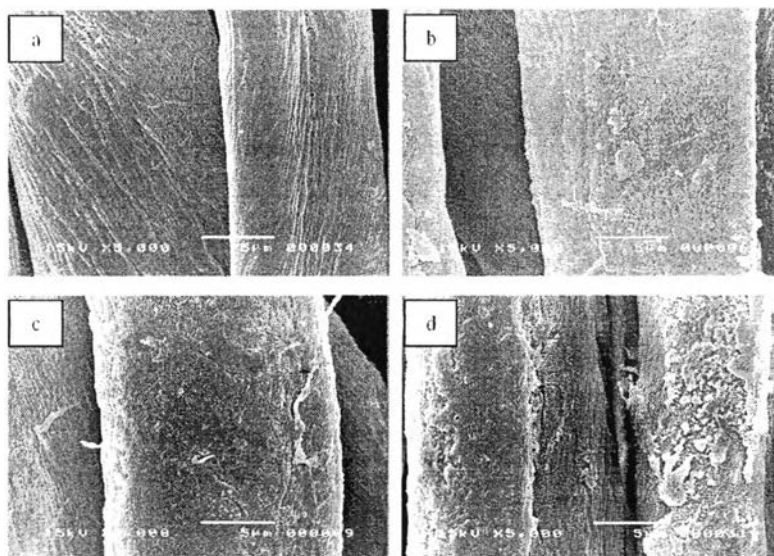


Figure 4.22 The effect of DBD plasma treatment time on the surface roughness of muslin fabric, (a) non DBD plasma treated fabric, (b-d) DBD plasma treated fabric 30 seconds, 2 min and 3 min, respectively.

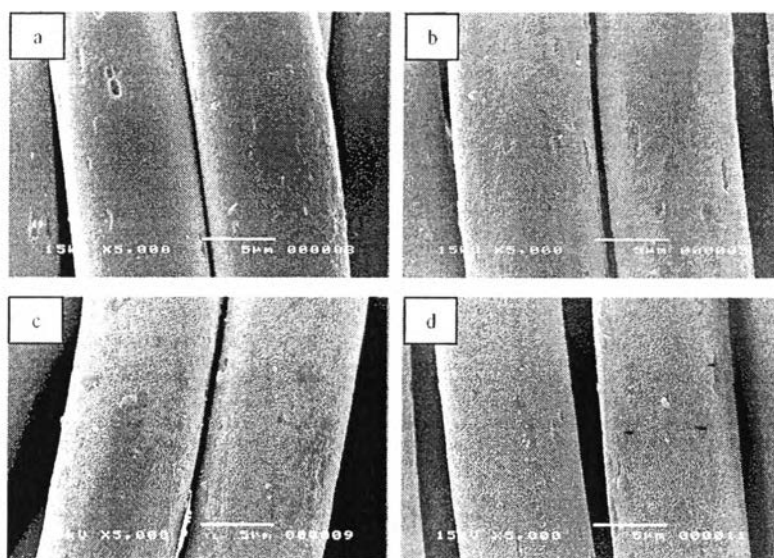


Figure 4.23 The effect of DBD plasma treatment time on the surface roughness of polyester fabric, (a) non DBD plasma treated, (b-d) DBD plasma treated fabric 30 seconds, 2 min and 3 min, respectively.

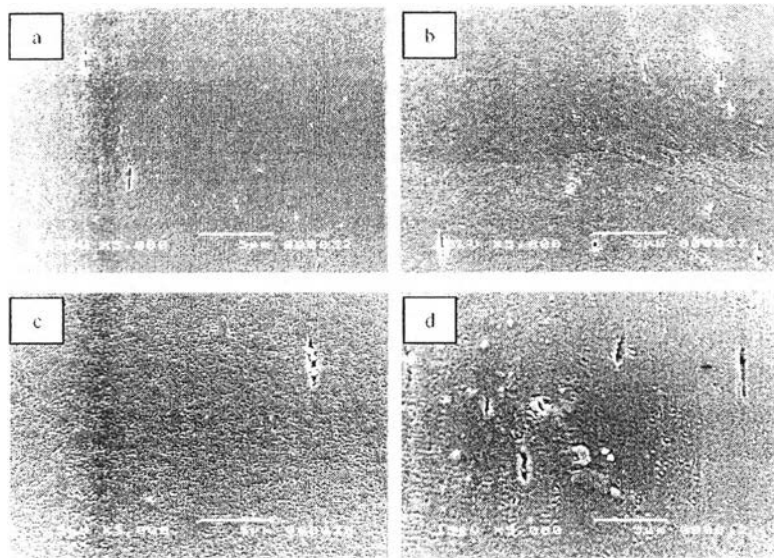


Figure 4.24 The effect of DBD plasma treatment time on the surface roughness of nylon mesh fabric. (a) non DBD plasma treated fabric, (b-d) DBD plasma treated fabric 30 seconds, 2 min and 3 min, respectively.

DBD plasma treated fabrics 2 minutes before cultivation in culture medium, the surface and cross section morphology of BC composites as shown in figure 4.25 and figure 4.26, respectively. The cross section morphology (figure 4.26 a-f), the interaction between bacterial cellulose fibrils and fabrics were observed, the same as BC composites containing non DBD plasma treated fabric. For each composites, the surface morphology (figure 4.25) and cross sectional morphology (figure 4.26 g-l) were the same as those of pure BC and BC composites containing non DBD plasma treated fabric but the fibrillar structures in the BC composites containing DBD plasma treated fabric were denser than that of pure BC and BC composites containing non DBD plasma treated fabric, especially in the BC/Nylon composites. From the results, explained that surface roughness of fabrics increased by DBD plasma treatment led to increase the number of cell attachment on fabrics more than that in BC composites containing non DBD plasma treated fabric and lead to increase production of fibrils, then the fibrillar structures were denser.

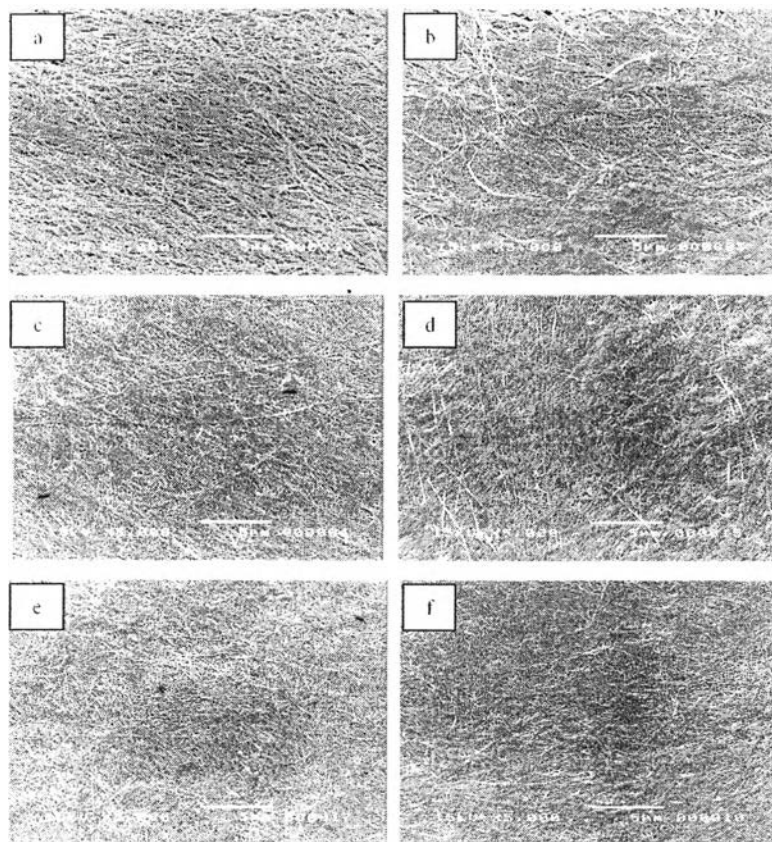
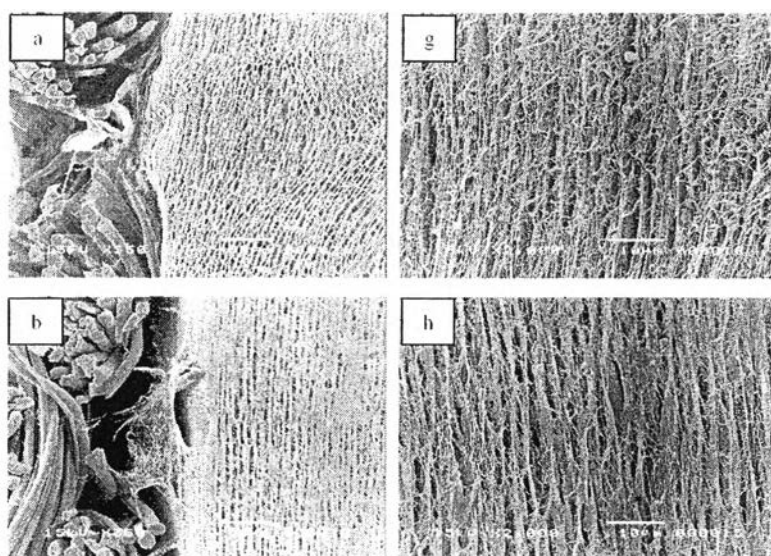


Figure 4.25 Surface morphology of (a) BC/Lenin, (b) BC/Cotton, (c) BC/Filter cloth, (d) BC/Muslin, (e) BC/Polyester and (f) BC/Nylon composites, respectively (DBD plasma treated fabrics 2 minutes before cultivation).



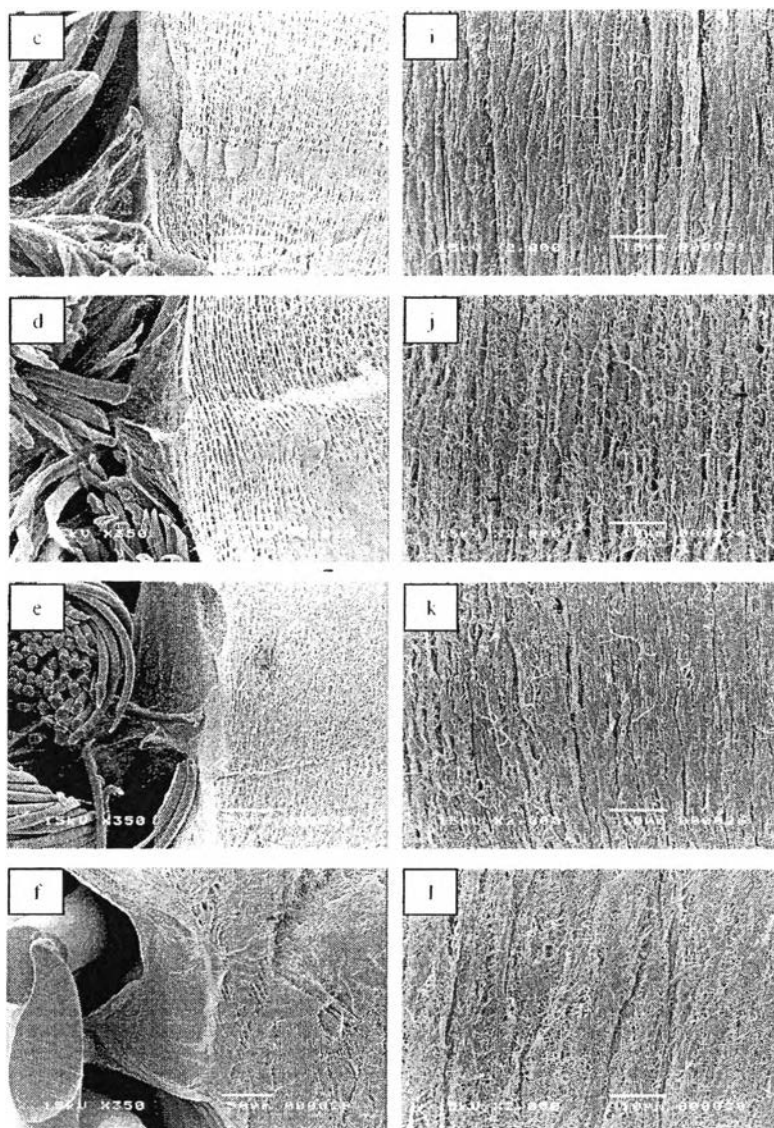


Figure 4.26 (a-f) shown cross sectional morphology and (g-l) shown only BC part in BC/Lenin, BC/Cotton, BC/Filter cloth, BC/Muslin, BC/Polyester and BC/Nylon, respectively (DBD plasma treated fabrics 2 minutes before cultivation).

4.6 Hydrophilicity of Fabrics

Regarding the analysis of FTIR spectra of untreated and treated fabrics, it was not identified significant variation in the spectra before and after DBD plasma treatment as shown in figure 4.27-4.32. Since plasma treatment works in a nanometer

scale, it is impossible to be detected by the FTIR analysis that works in a micrometric scale.

Wicking properties were used to evaluate hydrophilicity of the fabrics. A fabric strip (10 mm x 80 mm) was suspended vertically above the colored distilled water surface in a glass beaker in a way that vertical bottom edge slightly touches the colored water. A spontaneous wicking occurs due to capillary force. The liquid absorption time was recorded when the height of liquid was 20 mm. Fabrics were measured how many second it took the moisture to travel 20 mm. A shorter absorption time indicate greater wicking capabilities. Figure 4.33 shows the comparison of wicking abilities between non DBD plasma treated fabric and DBD plasma treated fabrics. From the result, lenin, cotton, filter cloth and muslin, the absorption time of DBD plasma treated fabric have lower than non DBD plasma treated fabrics. Non DBD plasma treated polyester fabric not shows the vertical wicking ability during the test due to the lower water absorption ability of polyester fabric. After DBD plasma treatment, polyester fabric shows the vertical wicking ability. This behavior is due to DBD plasma treatment introduce the polar functional groups on the surface of fabrics leading to increase hydrophilicity of fabrics that explained by shorter water absorption time. However, nylon mesh fabric not shows the vertical wicking ability both non DBD plasma treated fabric and DBD plasma treated fabric due to the surface of nylon mesh was shiny and lower water absorption ability. DBD plasma treatment might be not improved hydrophilicity, it might be improved only the surface roughness of fabrics as shown in section 4.5.

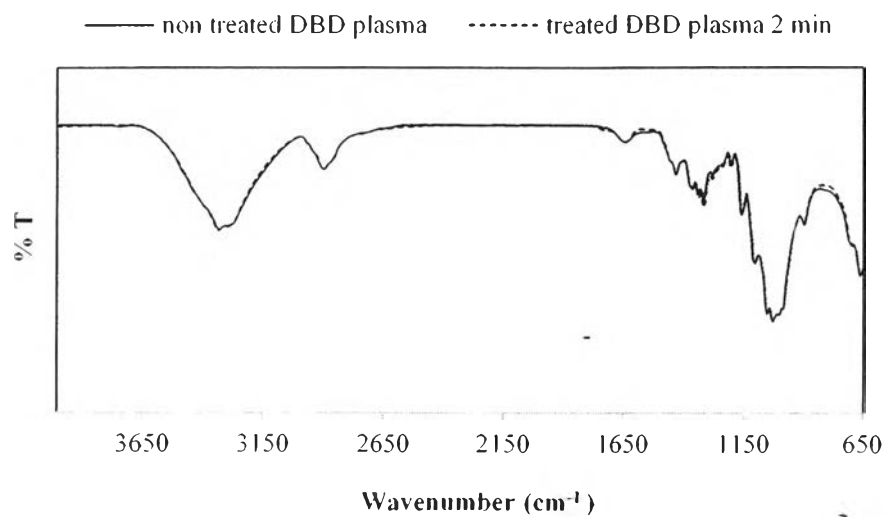


Figure 4.27 Comparison FTIR spectra of lenin fabric between non DBD plasma and DBD plasma treated fabric 2 min.

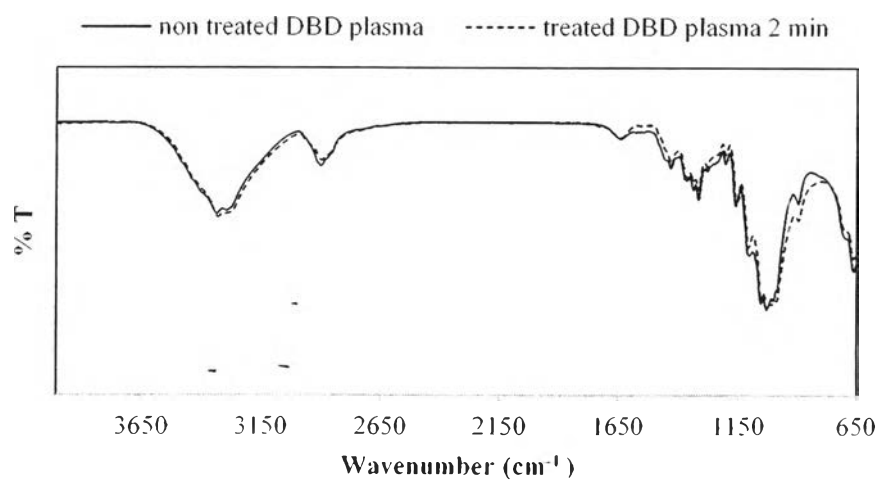


Figure 4.28 Comparison FTIR spectra of cotton fabric between non DBD plasma and DBD plasma treated fabric 2 min.

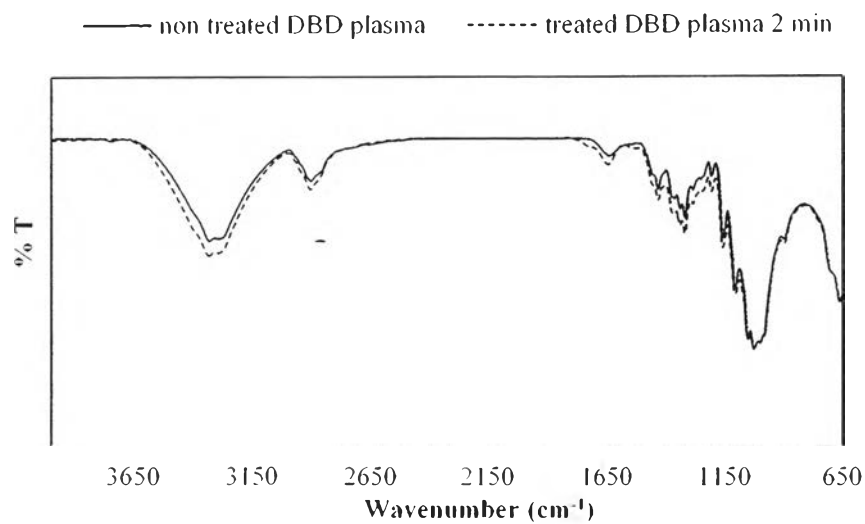


Figure 4.29 Comparison FTIR spectra of filter cloth fabric between non DBD plasma and DBD plasma treated fabric 2 min.

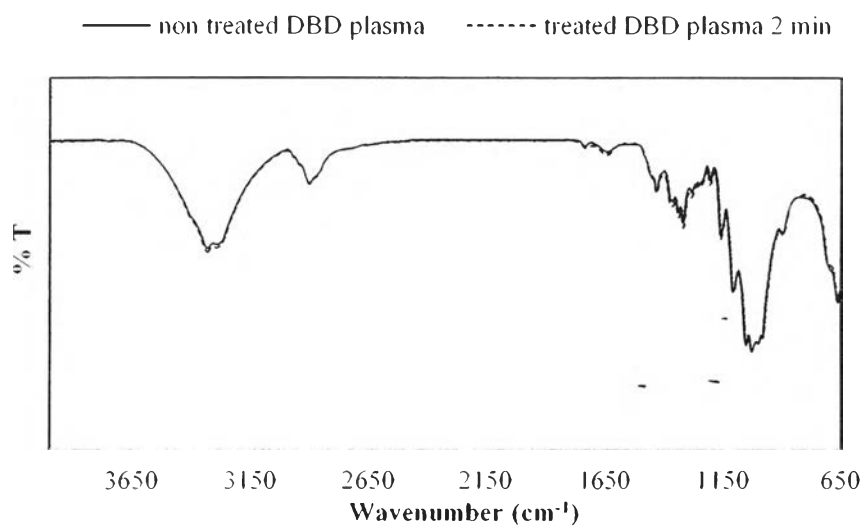


Figure 4.30 Comparison FTIR spectra of muslin fabric between non DBD plasma and DBD plasma treated fabric 2 min.

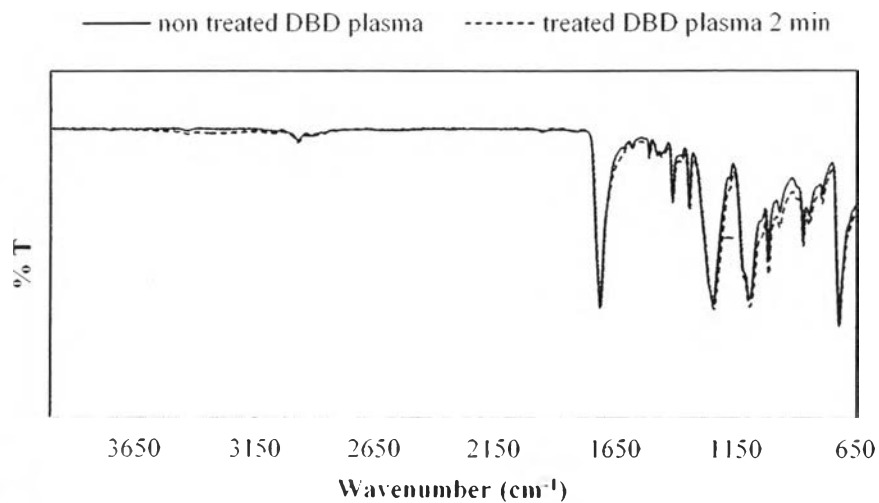


Figure 4.31 Comparison FTIR spectra of polyester fabric between non DBD plasma and DBD plasma treated fabric 2 min.

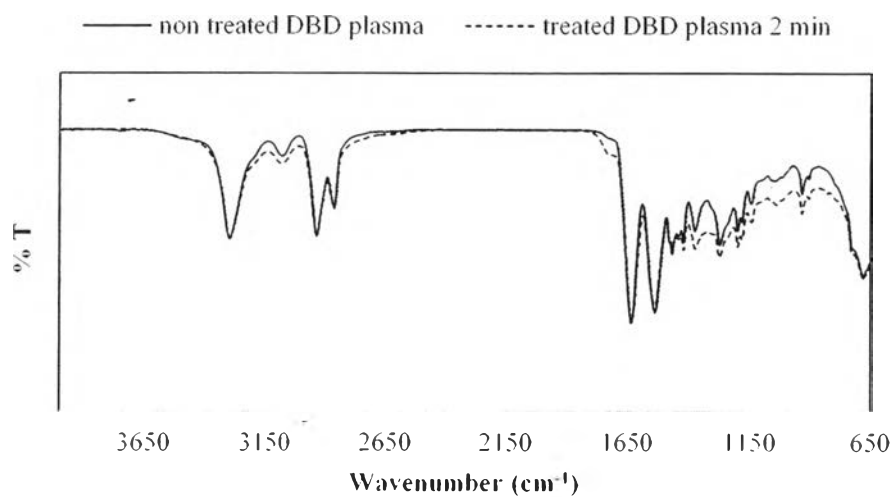


Figure 4.32 Comparison FTIR spectra of nylon mesh fabric between non DBD plasma and DBD plasma treated fabric 2 min.

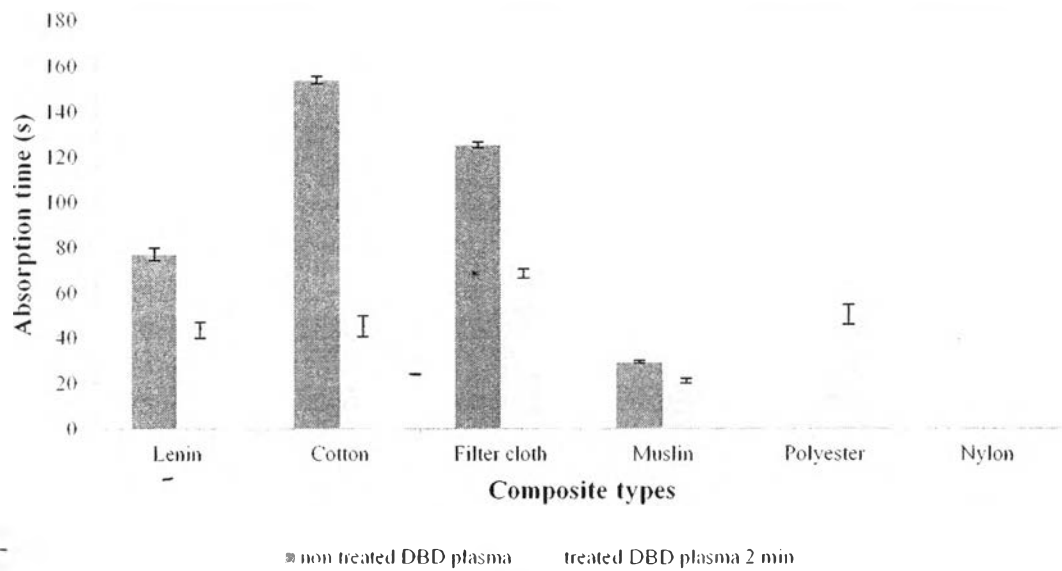


Figure 4.33 Comparison of wicking abilities between non DBD plasma and DBD plasma treated fabrics. (n=3)

4.7 Production Yields of BC Composites

The production yields of BC composites were calculated from dry weight of bacterial cellulose on fabrics. The production yields of DBD plasma treatment fabrics composites were increased when compared with pure BC and BC composites containing non DBD plasma treated fabric as shown in figure 4.34. From this result, explained that the fibrillar structures were denser, dry weight of BC were higher.

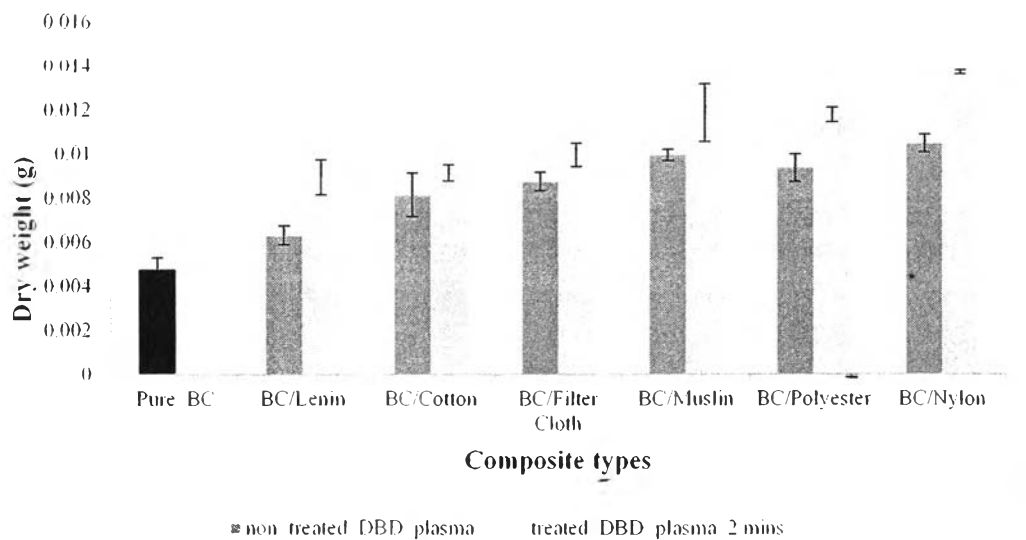


Figure 4.34 The comparison of production yields of pure BC and BC composites containing non DBD plasma treated fabrics and DBD plasma treated fabrics 2 min (cultivation time 2 days, n=3).

4.8 Mechanical Properties

In a large scale production of BC pellicles, damage from tearing of BC pellicle may occur during cultivation, sterilization, and packing into packaging. In order to reinforce BC pellicles, BC composites consisting of fabric embedded in the BC pellicles were fabricated. Tensile strength of BC composites containing non DBD plasma treated fabrics were increased both in wet and dried state, compared with that of pure BC, as shown in figure 4.35. The tensile strength of each sample depended on the type of fabrics. High tensile strength of fabrics led to higher tensile strength of BC composites as shown in figure 4.36. For each samples, tensile strength in wet state lower than those in dried state because density of hydrogen bonding between nanofibrils of samples in wet state was lowered that results from the penetration of the water molecules into the network of nanofibrils, then the nanofibrils mobility was increased resulting in the lower tensile strength. The samples in dried state have high density of hydrogen bonding of nanofibrils, that inhibited the motion of nanofibrils.

However, the tensile strength of DBD plasma treated fabrics was decreased compared with non DBD plasma treated fabrics especially lenin, cotton, filter cloth and muslin fabrics. The cause may be DBD plasma etching the surface of fabrics damaged the structure of fabrics leaded to decrease tensile strength as shown in figure 4.36.

In wet state, tensile strength of BC composites containing DBD plasma treated fabrics. BC/Lenin, BC/Cotton and BC/Muslin, were decreased compared with that of BC composites containing non DBD plasma treated fabrics due to fabrics loss the strength from DBD plasma treatment. For BC/filter cloth, the tensile strength of composites containing DBD plasma treated fabrics was not difference from composites containing non DBD plasma treated fabrics. In contrast, BC/Polyester and BC/Nylon, the tensile strength of composites containing DBD plasma treated fabrics were increased although the tensile strength of DBD plasma treated fabrics was decreased. The cause may be the morphology of fibrils of BC composites containing DBD plasma treated fabrics denser than another BC composites containing DBD plasma treated fabrics (section 4.5) and the tensile strength of DBD plasma treated polyester and nylon mesh fabrics higher than other DBD plasma treated fabrics as shown in figure 4.36. Both of them can be improved the strength of composites.

In dry state, the tensile strength of BC composites containing DBD plasma treated fabrics were increased compared with BC composites containing non DBD plasma treated fabrics and pure BC, except BC/Lenin. The cause may be the morphology of fibrils of BC composites containing DBD plasma treated fabrics were denser and it have high density of hydrogen bonding of nanofibrils, that inhibited the motion of nanofibrils the same as BC composites containing non DBD plasma treated fabrics in dry state. Then, the tensile strength of BC composites was increased, although tensile strength of fabrics was decreased due to damaged from DBD plasma.

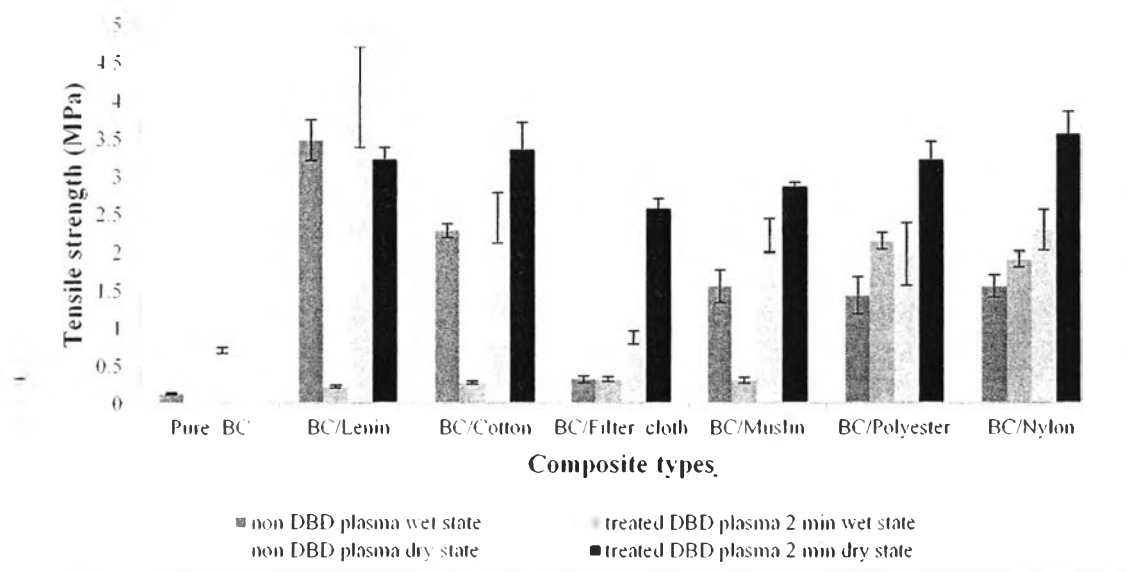


Figure 4.35 The comparison of tensile strength of pure BC and BC composites containing non DBD plasma treated fabrics and DBD plasma treated fabrics 2 min both wet and dry state. (n=5)

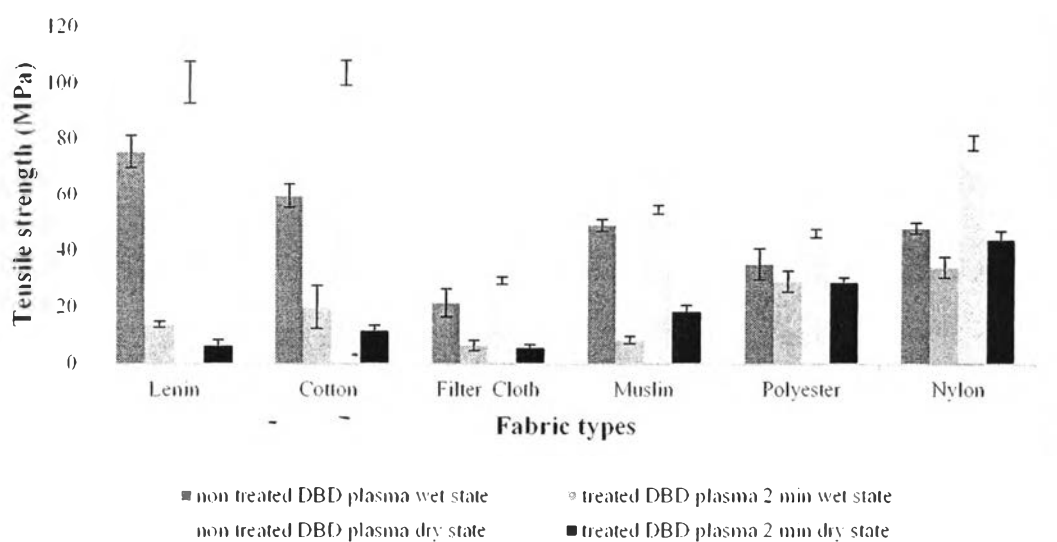


Figure 4.36 The comparison of tensile strength of non DBD plasma treated fabrics and DBD plasma treated fabrics 2 min both wet and dry state. (n=5)

4.9 Water Absorption Capacity (WAC)

Water absorption capacity plays an important role in wound dressing application. The capacity of absorbing wound exudates and maintaining moist environment at wound surface are important factors in wound healing process. Bacterial cellulose has high water absorption capacity due to the hydrophilicity and porous structure of nanofibril network. The porous structure of bacterial cellulose generated the high surface areas and capillary force which enhancing the water absorption capacity. Using porous supporting fabrics, water absorption capacity of BC composites were decreased, compared with that of pure BC as shown in figure 4.37. It might be explained that tightly packing fibrillar structure in the BC composites restricted of the swelling behavior of BC.

From figure 4.37, the result shows that the swelling behavior of BC depends on the morphology of BC for each composite. The morphology of bacterial cellulose of BC/Nylon denser than other BC composites (as shown in section 4.4), then it has lower swelling behavior.

In addition, the comparison on the water absorption capacity between BC composites containing non DBD plasma treated fabrics and DBD plasma treated fabrics, it was found that DBD plasma treatment resulted in lowering of the swelling ratios. Because the morphology of BC composites containing DBD plasma treated fabrics denser than BC composites containing non DBD plasma treated fabrics, then it more restricted of the swelling behavior of BC. However, both BC composites containing non DBD and DBD plasma treated fabrics not loss absorption ability.

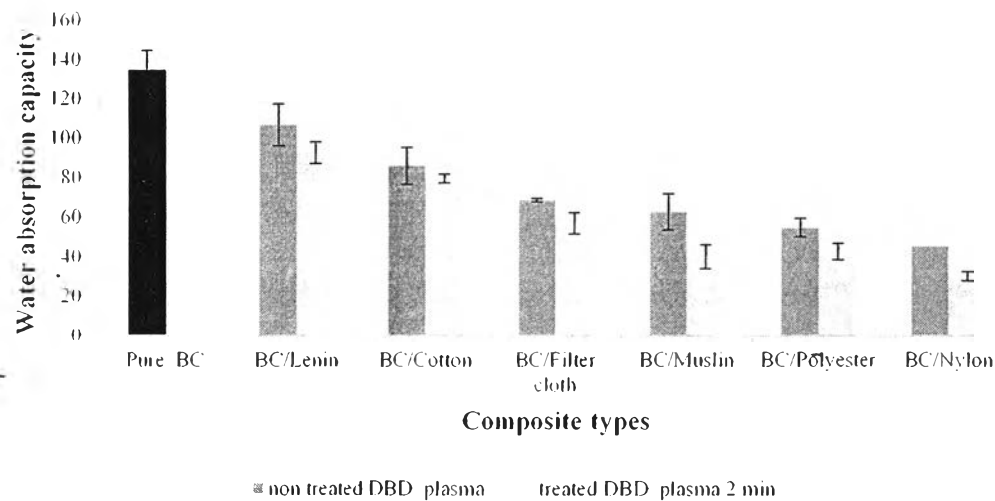


Figure 4.37 The comparison of water absorption capacity of pure BC and BC composites containing non DBD plasma treated fabrics and DBD plasma treated fabrics 2 min. (n=3)

4.10 Water Vapor Transmission Rate (WVTR)

The WVTR has been identified as an effective and objective indicator of the moisture-retention capacity of various dressing. The low WVTR is a reliable indicator of a dressing's capacity to retain moisture and thus to provide an environment that supports healing (Brett, 2006).

The WVTR of pure BC was 993.82 g/m²/day, as shown in figure 4.38. BC composites with different fabric types had different values of WVTR. The values of WVTR of BC composites depend on fabric types as shown in figure 4.39. The water vapor transmission rate of BC composites was in the range of commercial wound dressing (308-2892 g/m²/day) (Wu P. *et al.*, 1995). The WVTR of BC/Lenin, BC/Cotton, BC/Muslin and BC/Nylon composites were not different from that of pure BC, although the cultivation time to produce BC composites was 2 days, while the cultivation time to produce pure BC was 4 days. It might be explained that the tightly packing fibrillar structure in the BC composites reduced the mobility of water molecules throughout the BC matrix, resulting in the reduction of WVTR. For BC/Polyester and BC/Filter cloth, the WVTR higher than pure BC and other BC

composites due to the high WVTR of polyester fabric and filter cloth, then it might be effect on WVTR of BC composites. Compared with pure BC with the comparable WVTR, BC composites can be produce with the shorter cultivation time, leading to the lower production cost.

Moreover, DBD plasma treatment can reduce WVTR, compared with BC composites containing non DBD plasma treated fabrics, as shown in figure 4.38. The WVTR of BC composites containing DBD plasma treated fabrics was reduced due to the more tightly packing of fibrilar structure of BC composites as shown in section 4.5.

However, there is not exact ideal value of WVTR for wound dressing materials. If the WVTR is too high, it causes excessive dehydration which will create dry condition around wound area and result in scar formation. In contrast, if the WVTR is too low, this may lead to the delay of the healing process and the increasing of bacterial growth due to the accumulation of exudates. Water vapor transmission rate (WVTR) of wound dressing should be controlled at an appropriate rate. Recently, it has been reported that wound healing takes place faster in moist environment (Bhuvanesh G., 2010). For moist wound environment, the effect of moisture on epidermal regeneration included enhanced keratinocyte migration, proliferation and differentiation. In addition, moisture promoted fibroblast proliferation, collagen synthesis, endothelial cell proliferation, new vessel formation (angiogenesis) and wound contraction. A moist wound healing environment is associated with each of the following : (1) shorter and less intense inflammatory phase, (2) earlier proliferation, migration and differentiation of keratinocyte, (3) enhanced fibroblast proliferation and collagen synthesis and (4) earlier wound contraction. Wound contraction and reduction in wound surface area are strong predictors of wound healing (Brett, 2006).

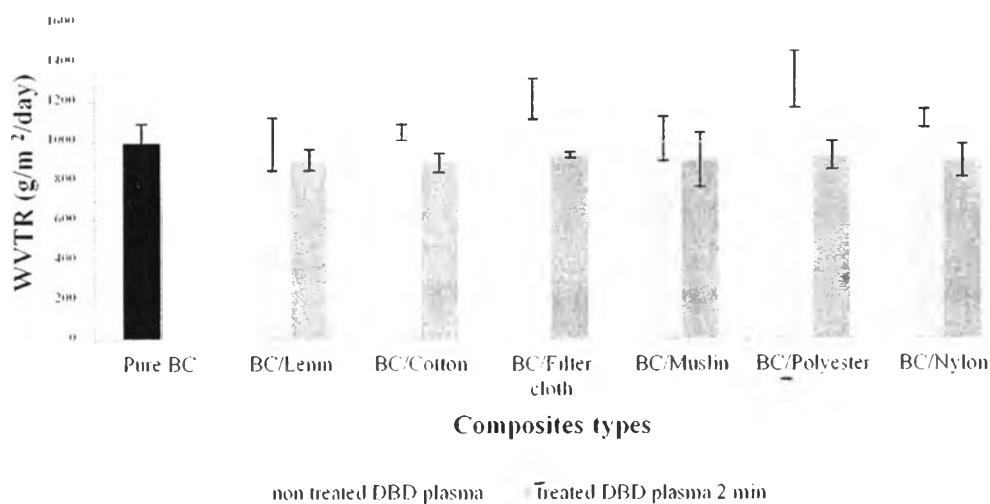


Figure 4.38 The comparison of water vapor transmission rate of pure BC and BC composites containing non DBD plasma treated fabrics and DBD plasma treated fabrics 2 min. (n=3)

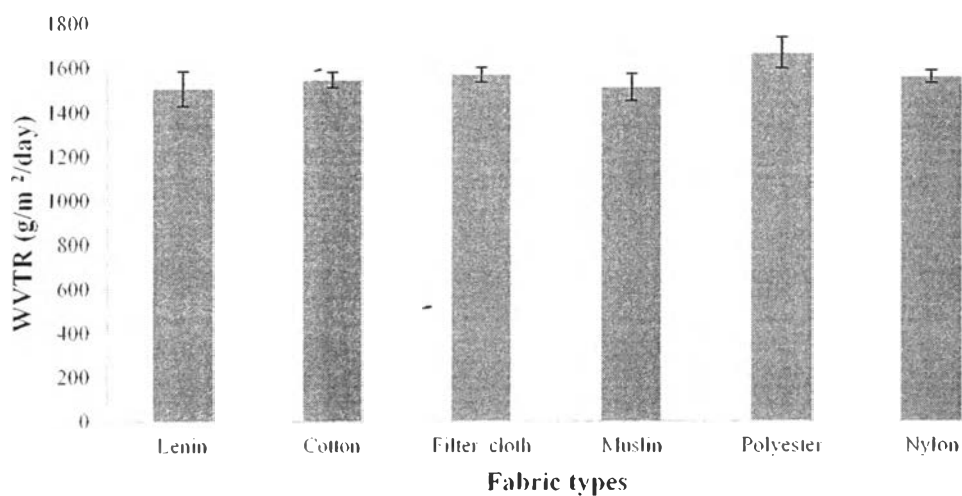


Figure 4.39 The comparison of water vapor transmission rate of fabrics. (n=3)

4.11 The In Vivo Experiment

This experiment was approved by the national laboratory animal center (NLAC) Mahidol University. Twenty four male rats (Sprague Dawley), Each rat was 8-9 weeks old, weighting approximately 280-300 g, were used in this study. The rats were kept in separate cages at a temperature of 22 C in a light dark cycle of 12 hours for 3 days prior to the experiment. They were had unlimited supply for food and drinking water.

The hair on the back of each of the rats was removed. The rats were anaesthetized with isofluran 3-4 %. All surgical procedures were performed under strict aseptic protocol. Each animal were made four incision of 6 mm in diameter with biopsy puncher and distance of approximately 1 mm among them as shown in figure 4.40

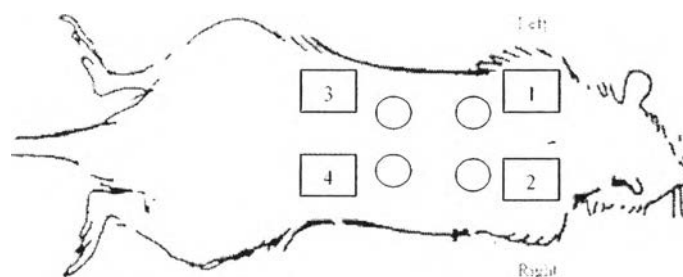


Figure 4.40 Identification of the wound created surgically for the respective treatment groups.

Position 1-3, pure BC, BC/Cotton and BC/Nylon composites were put on the wound, respectively. Position 4, 3M tegraderm film 1624W was put on the wound as the controls.

Pure BC, BC/Cotton, BC/Nylon were used to study their effect on wound healing in rat models compared with 3M tegraderm film 1624W that is the commercial wound dressing as shown in figure 4.41.

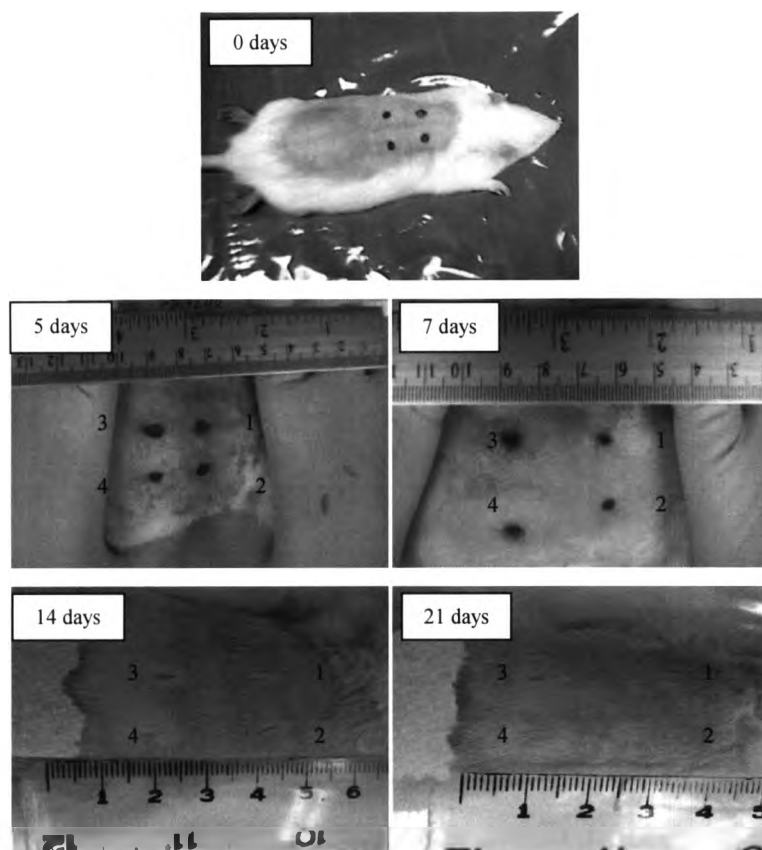


Figure 4.41 Image of wound in rats (position 1) pure BC, (position 2) BC/cotton, (position 3) BC/Nylon and (position 4) 3M tegraderm film 1624W at 0,5,7,14 and 21days.

At fifth days, the epithelialization at wound site was observed. Wound treated with pure BC contracted faster than other groups. The percent of wound contraction as shown in figure 4.42, the percent of wound contraction of pure BC higher than other groups. Apparently, wound treated with pure BC healed more rapidly, as compared with those treated with BC/Cotton, BC/nylon and 3M tegraderm film 1624W (the controls), that is the commercial wound dressing. However, BC/Cotton was no significant difference in the percent of wound contraction compared with pure BC and 3M tegraderm film 1624W that used as the controls. BC/Nylon has lower the percent of wound contraction compared with other groups. Wound treated with pure BC and BC composites healed more rapidly because the well organized network structure of BC exhibited the effective exudation

absorption capacity for wounds. In addition, BC membranes have better the tissue regeneration of wound during wound treatment (Wen C.L. *et al.*, 2013). However, wound completely healed after 14 days for all groups and not observed the scar formation in the wound sites.

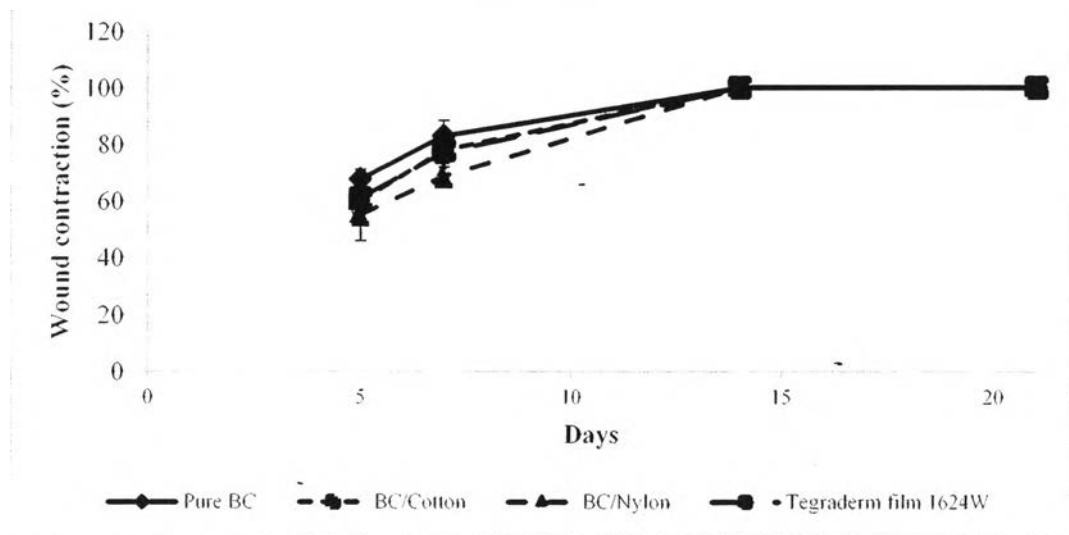


Figure 4.42 Comparison the percent of wound contraction during the wound healing, 5 days (n=24), 7 days (n=18), 14 days (n=12) and 21 days (n=6).

The thickness of BC can be effect on wound healing process. wound healed more rapidly in thick BC (Kan, C.W. *et al.*, 2012). Using longer cultivation time, the higher thickness of BC was obtained. In this research, the cultivation time of pure BC was 4 days, while the cultivation of BC composites was 2 days. Wound treated with pure BC contracted faster than other groups, the cause may be it has higher thickness. However, it could be suggested that pure BC and BC composites have a good potential in wound healing.

The appropriate wound dressing is BC/Cotton. BC/Cotton was no significant difference in the percent of wound contraction compared with pure BC and 3M tegraderm film 1624W that used as the controls, especially, BC/Cotton can be produce with the shorter cultivation time. leading to the lower production cost.

Figure 4.43 shows the body weight of rats during the wound healing at 5, 7, 14 and 21 days. The body weight of rats was no significant difference during wound healing. In addition, figure 4.44 and 4.45 show the food consumption and water consumption of rats, respectively. From the results, there was no significant difference in food and water consumption of rats. Then, it could be suggest that pure BC and BC composites was not in vivo toxicity in wound healing.

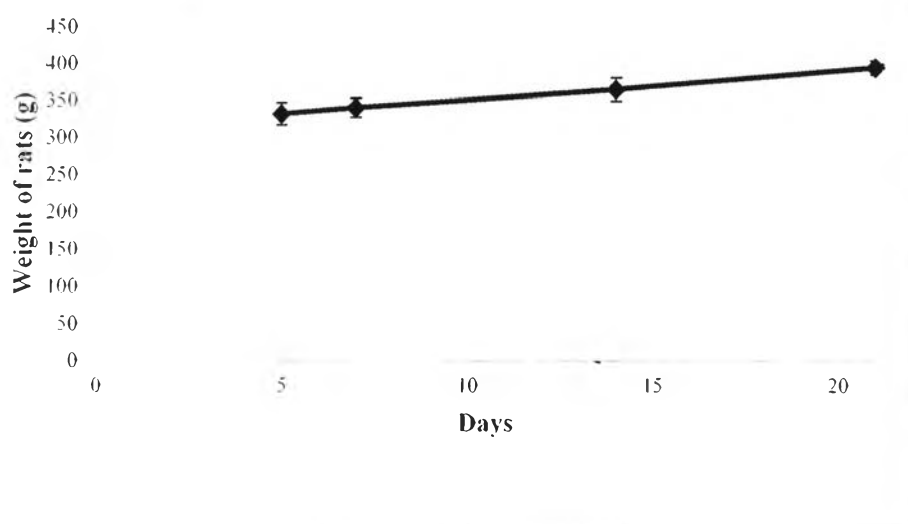


Figure 4.43 The body weight of rats during the wound healing.

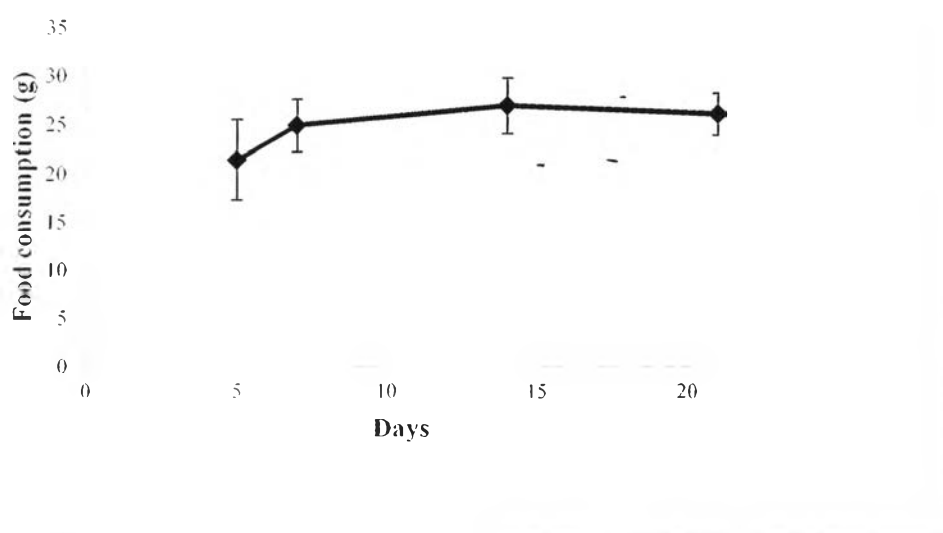


Figure 4.44 The food consumption of rats during the wound healing.

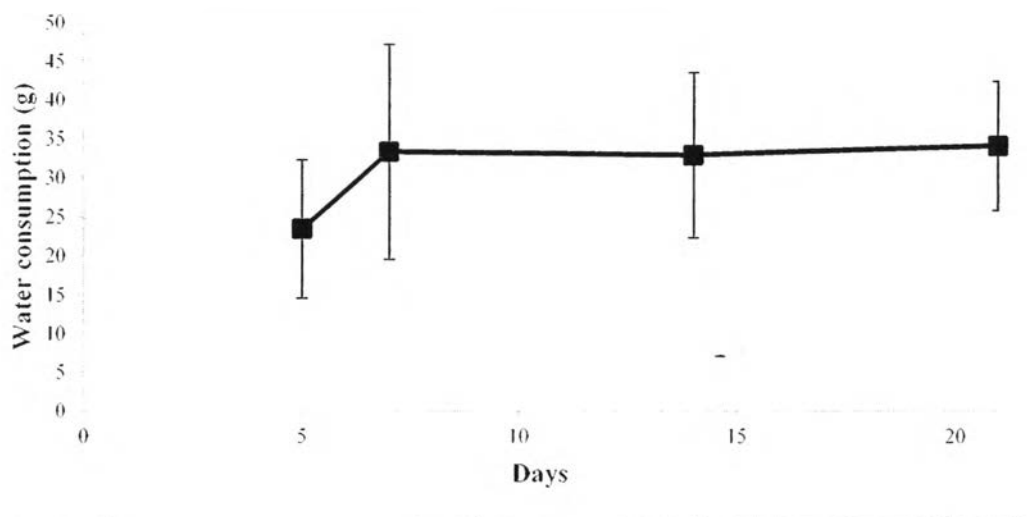


Figure 4.45 The water consumption of rats during the wound healing.

4.12 The In Vitro Experiment

This experiment was approved by National Center for Genetic Engineering and Biotechnology; (BIOTEC, NSTDA). The biocompatibility is one of the important factors during wound treatment. MTT assay is colorimetric assay for measuring the activity of enzymes from metabolism of cells. This assay was a modified version of conventional direct and indirect contact tests conformed to the published standard methods (BS-EN30993-5 and ISO10993-5). The MTT assay is a tetrazolium-dye based colorimetric microtitration assay. Metabolism-competent cells are able to metabolize the tetrazolium (yellow) to formazan (blue); this color change is measured spectrophotometrically with a plate reader. It is assumed cells that are metabolically deficient will not survive, thus the MTT assay is also an indirect measurement of cell viability.

The percent survival of the human dermal skin fibroblast cells cultured with samples (compared to control) shown in figure 4.46

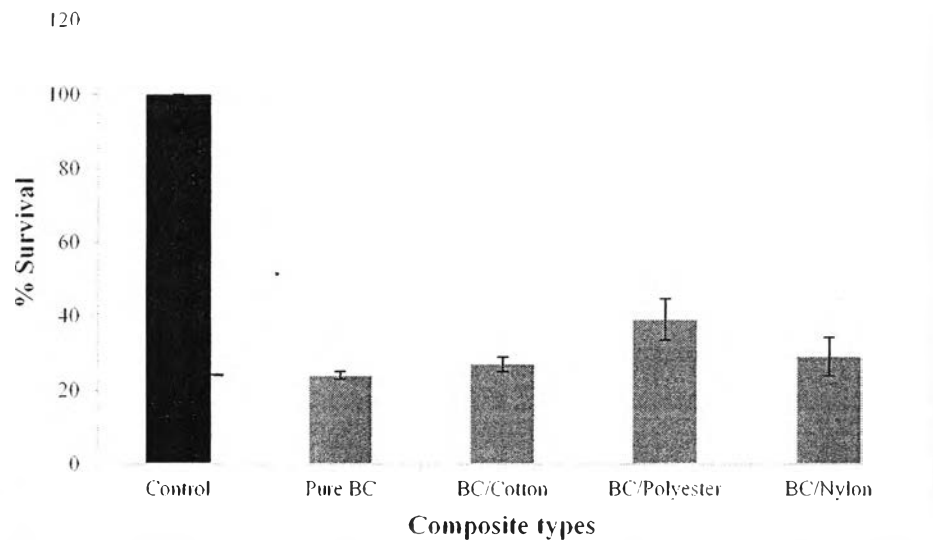


Figure 4.46 The percent survival of human dermal skin fibroblast cell lines. (n=3)

The percent survival of human dermal skin fibroblast cells cultured with BC composites: BC/Cotton, BC/polyester and BC/Nylon, more than pure BC. However, based on the percent survival of each test concentration, the toxicity of sample can be indicated as: a) "non-cytotoxic effect" if cell survived $>50\%$ and b) "cytotoxic effect" if cell survived $<50\%$. Then, Pure BC, BC/Cotton, BC/Polyester and BC/Nylon were cytotoxic to human dermal skin fibroblast cell lines showed by the percent survival less than 50%. The contamination of fungus occurs during the experiment, it may be effect on the percent survival of cells.

SEM images of the cell attachment of human dermal skin fibroblast cells on Pure BC, BC/Cotton, BC/Polyester and BC/Nylon as shown in figure 4.47. In generally, the cells spread on the surface and stretched their morphology indicated that the materials show the better biocompatibility. In this experiment, there were many cells attached on each material but the cells remained in the round shape, it not stretched the morphology. The contamination of fungus during the experiment, it may be effect on the cell attachment and cell growth.

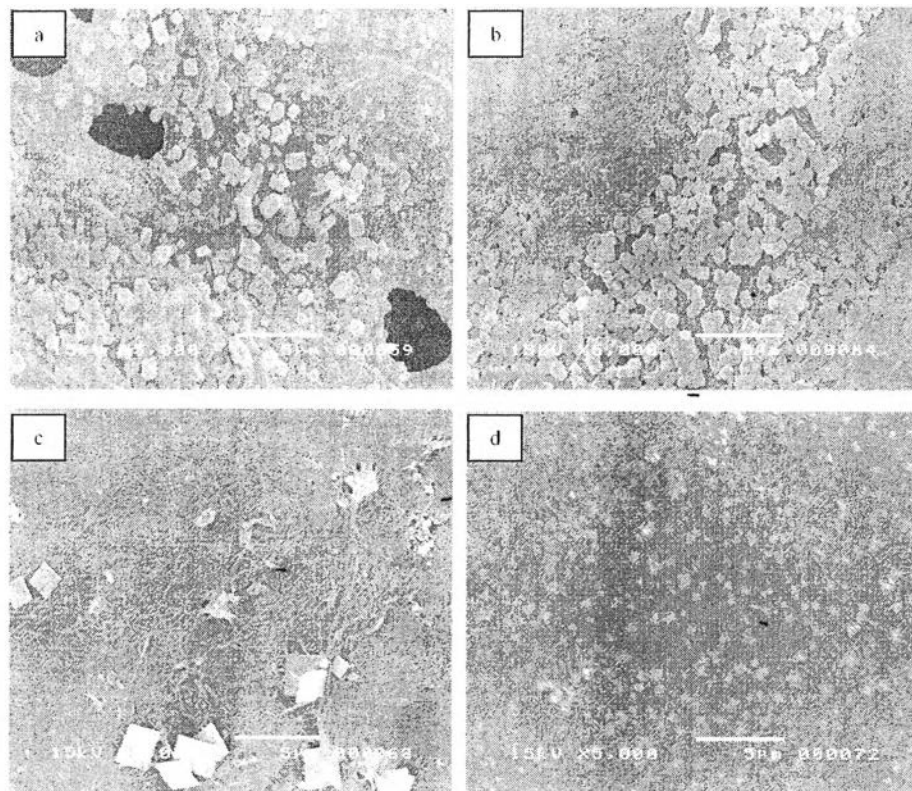


Figure 4.47 Cell attachment of human dermal skin fibroblast on (a) pure BC, (b) BC/Cotton, (c) BC/Polyester and (d) BC/Nylon, respectively.